The Plant Cell, Vol. 24: 215–232, January 2012, www.plantcell.org

Routes to the Tonoplast: The Sorting of Tonoplast Transporters in *Arabidopsis* Mesophyll Protoplasts [W]

Susanne Wolfenstetter, Petra Wirsching, Dorina Dotzauer, Sabine Schneider, and Norbert Sauer[1]

Friedrich-Alexander-Universität Erlangen-Nürnberg, Molecular Plant Physiology and ECROPS (Erlangen Center of Plant Science), D-91058 Erlangen, Germany

Vacuoles perform a multitude of functions in plant cells, including the storage of amino acids and sugars. Tonoplast-localized transporters catalyze the import and release of these molecules. The mechanisms determining the targeting of these transporters to the tonoplast are largely unknown. Using the paralogous *Arabidopsis thaliana* inositol transporters INT1 (tonoplast) and INT4 (plasma membrane), we performed domain swapping and mutational analyses and identified a C-terminal di-leucine motif responsible for the sorting of higher plant INT1-type transporters to the tonoplast in *Arabidopsis* mesophyll protoplasts. We demonstrate that this motif can reroute other proteins, such as INT4, SUCROSE TRANSPORTER2 (SUC2), or SWEET1, to the tonoplast and that the position of the motif relative to the transmembrane helix is critical. Rerouted INT4 is functionally active in the tonoplast and complements the growth phenotype of an *int1* mutant. In *Arabidopsis* plants defective in the β-subunit of the AP-3 adaptor complex, INT1 is correctly localized to the tonoplast, while sorting of the vacuolar sucrose transporter SUC4 is blocked in *cis*-Golgi stacks. Moreover, we demonstrate that both INT1 and SUC4 trafficking to the tonoplast is sensitive to brefeldin A. Our data show that plants possess at least two different Golgi-dependent targeting mechanisms for newly synthesized transporters to the tonoplast.

INTRODUCTION

Vacuoles are the largest plant organelles, constituting up to 90% of the cell volume. They are indispensable for multiple cellular functions, including the maintenance of turgor to shape the individual cell and the entire plant; the storage of anthocyanins for flower coloration or during light stress; the accumulation of toxins, such as glucosinolates or opiates, to keep herbivores at bay; the concentration of ions needed for cellular signaling (Ca^{2+}) or metabolism (e.g., NO_3^- or SO_4^{2-}); and the storage of sugars or amino acids to withstand low temperatures or to survive unfavorable environmental conditions. All of these vacuolar functions depend on the tightly regulated activities of numerous tonoplast-localized transporters and channels (Martinoia et al., 2007; Neuhaus, 2007; Isayenkov et al., 2010). For many of these proteins (e.g., for the tonoplast-localized transporters for inositol [INOSITOL TRANSPORTER1 (INT1); Schneider et al., 2008], Glc [TONOPLAST MONOSACCHARIDE TRANSPORTER1 (TMT1) and TMT2; Wormit et al., 2006], or Suc [SUC TRANSPORTER4 (SUC4); Schulz et al., 2011]), paralogous transporters are found in the plasma membrane. Obviously, the tonoplast transporters and their plasma membrane paralogs possess conserved core-domains for their specific catalytic functions but variable sorting domains for intracellular targeting. So far, however, little is known about these sorting motifs and about the mechanisms involved in the differential targeting of paralogous transporters to their respective membranes.

Sorting motifs may be recognized by the COPI or COPII complexes for retrograde or anterograde transport between the endoplasmic reticulum (ER) and the Golgi (Hanton et al., 2005a; Hwang and Robinson, 2009) or by ADAPTOR PROTEIN (AP) complexes, some of which link their cargo proteins to clathrin (reviewed in Kirchhausen, 1999; Bonifacino and Traub, 2003; Robinson, 2004). The resulting clathrin-coated vesicles are involved in membrane protein endocytosis and in post-Golgi traffic (Bonifacino and Traub, 2003; Hwang and Robinson, 2009; Foresti et al., 2010; Pandey, 2010). AP complexes are heterotetramers and were studied intensively in animals (four complexes: AP-1 to AP-4) and *Saccharomyces cerevisiae* (three complexes: AP-1 to AP-3; Bonifacino and Traub, 2003; Robinson, 2004). In animals, AP-1 is involved in cargo shuttling between the trans-Golgi network (TGN) and the endosomes, AP-2 in endocytosis from the plasma membrane, AP-3 in protein trafficking to lysosomes and lysosome-related organelles, and AP-4 in sorting from the TGN to different membranes (Robinson, 2004). AP-1 and AP-2 bind clathrin, but AP-4 does not, and clathrin binding by AP-3 is under debate. In *Arabidopsis thaliana*, genes for the subunits for four putative AP complexes have been identified (Bassham et al., 2008), and evidence has been provided that the plant AP-2 complex is also involved in the recycling of proteins from the plasma membrane (Ortiz-Zapater et al., 2006; Dhonukshe et al., 2007).

Among the signals recognized by AP complexes, Tyr-based sorting signals (YXXØ, with X being any amino acid and Ø an amino acid with a bulky hydrophobic residue) and di-Leu–type sorting signals, [D/E]XXXL[L/I]-type sequences, were identified and characterized in yeast and animals (Bonifacino and Traub,

[1] Address correspondence to nsauer@biologie.uni-erlangen.de.
The author responsible for distribution of materials integral to the findings presented in this article in accordance with the policy described in the Instructions for Authors (www.plantcell.org) is: Norbert Sauer (nsauer@biologie.uni-erlangen.de).
[W] Online version contains Web-only data.
www.plantcell.org/cgi/doi/10.1105/tpc.111.090415

2003; Robinson, 2004; Pandey, 2010). Both types of signals are typically found in the C-terminal parts of sorted proteins but less frequently also in other regions, and the distance between these sequences and the adjacent transmembrane helix is critical for their signaling function (Bonifacino and Traub, 2003). For both motifs, the specificity of recognition is defined by the X residues within the core sequence and by additional nearby residues. Other Tyr-based signals (NPXY) and other di-Leu–type signals (DXXLL) are recognized by different adaptors (Bonifacino and Traub, 2003; Robinson, 2004).

Sorting of membrane proteins may also be achieved by acidic cluster motifs (Bonifacino and Traub, 2003), which represent Asp and/or Glu-rich regions, such as DDEESESD in the mammalian VESICULAR MONOAMINE TRANSPORTER2, a member of the major facilitator superfamily (Waites et al., 2001). Phosphorylation of one or a few Ser or Thr residues within this region can trigger binding of the sorting protein PHOSPHOFURIN ACIDIC CLUSTER SORTING PROTEIN1 (Gu et al., 2001), which finally connects the cargo protein to an AP complex and mediates targeting to the TGN (Scott et al., 2003).

The targeting of membrane proteins is well characterized in yeast and animals, whereas little is known about sorting signals and mechanisms in higher plants. Diacidic motifs, often residing in the N terminus of membrane proteins, are required for ER release (Hanton et al., 2005b; Dunkel et al., 2008; Zelazny et al., 2009; Cai et al., 2011; Sorieul et al., 2011). However, little is known about sorting motifs responsible for intracellular targeting of membrane proteins. Three individual Tyr-based motifs in the intracellular loop region of the *Arabidopsis* boron transporter BOR1 were shown to be important for polar localization of BOR1 and for its recycling from the plasma membrane (Takano et al., 2010). Another Tyr motif was found in the cytosolic region of the vacuolar sorting receptor BINDING PROTEIN80 (BP80) and plays an important role for post-Golgi trafficking to the prevacuolar compartment (PVC; daSilva et al., 2006) and for the recycling of BP80 from the plasma membrane (Saint-Jean et al., 2010).

Additionally, di-Leu motifs in the N-terminal region of the monosaccharide transporter ERD SIX-LIKE1 (ESL1) (Yamada et al., 2010) and of the molybdate transporter MOT2 (Gasber et al., 2011) were shown to be responsible for the correct sorting of these transporters to the tonoplast.

In other studies, certain domains of membrane proteins were shown to be responsible for their tonoplast targeting. Examples are the tonoplast two pore K^+ channels (TPKs), which were shown to contain targeting information in their cytosolic C termini both in rice (*Oryza sativa*; Isayenkov et al., 2011) and *Arabidopsis* (Maîtrejean et al., 2011). For the tonoplast-localized syntaxin VESICLE-ASSOCIATED MEMBRANE PROTEIN711, an N-terminal longin domain was demonstrated to be necessary for its correct sorting (Uemura et al., 2005).

Here, we addressed the question of subcellular sorting using the paralogous *Arabidopsis* inositol transporters INT1 (tonoplast) and INT4 (plasma membrane; Schneider et al., 2006). Using domain swapping, mutational analyses, and confocal imaging of GREEN FLUORESCENT PROTEIN (GFP)-labeled chimera, we identified a C-terminal sorting motif in INT1 and demonstrated that this motif can be used to reroute plasma membrane and ER-localized transporters to the tonoplast. Rerouted INT4 complements an *int1* mutation, indicating that plasma membrane transporters are functionally active in the tonoplast. We finally demonstrate that INT1 and the tonoplast-localized Suc transporter SUC4 are sorted to the vacuole by different mechanisms and that the sorting motif from the INT1 C terminus can be used to sort SUC4 via the INT1 route.

RESULTS

The C-Terminal Domains of Plant Inositol Transporters Determine Their Subcellular Localization

To identify the protein domains required for transporter sorting, we conducted domain swap experiments on two *Arabidopsis* transporters with different subcellular localizations: the tonoplast-localized inositol transporter INT1 and the plasma membrane–localized inositol transporter INT4 (see Supplemental Figure 1 online). To obtain exchangeable *INT1* and *INT4* coding sequence (CDS) modules, unique restrictions sites (*Avr*II, *Nae*I, and *Stu*I) were introduced at identical positions into the *INT1* and *INT4* CDS (see Supplemental Figure 1 online). These modifications did not alter the INT1 or INT4 protein sequences but allowed domain swapping of the large central loops (L1 = INT1 loop; L4 = INT4 loop; Figure 1A) and of the C-terminal domains (C1 = INT1 C terminus; C4 = INT4 C terminus). Additional swapping of the N-terminal domains (N1 = INT1 N terminus; N4 = INT4 N terminus) was achieved by PCR. Chimeric sequences were fused to the open reading frame of GFP, put under the control of the *35S* promoter, and used to study the subcellular localizations of the different chimera in *Arabidopsis* mesophyll protoplasts by confocal microscopy. The names of the constructs indicate the position of GFP, the deleted transporter domain, and the origin of the inserted domain. For example, GFP-INT1ΔC(C4) describes an N-terminal GFP fusion to an INT1 protein that has its C terminus deleted and replaced by the C terminus of INT4. For all GFP fusions analyzed in this article, the distribution to different subcellular compartments (plasma membrane, tonoplast, ER, and Golgi) was determined in at least 50 protoplasts. For optimal detectability of tonoplast labeling, vacuoles were released from osmotically lysed protoplasts (e.g., right image in Figure 1B). All tested GFP fusions clearly localized to one specific compartment. However, some of the fusion proteins that were destined for the plasma membrane or the tonoplast gave a transient additional staining of the ER/Golgi. We believe that this additional signal came from newly synthesized proteins that had not been completely targeted yet. In some rare cases, chimeric proteins were not 100% rerouted to one single membrane and showed an additional staining of another compartment. In Supplemental Table 1 online, the relative staining intensities in the different compartments are summarized for every individual construct, discriminating between preferred, transient, and additional localization. To demonstrate that each of our constructs gives rise to an intact fusion protein that is stable in transiently transformed mesophyll protoplasts, we also performed immunoblot analyses using an anti-GFP antibody (see Supplemental Figure 2 online).

The inositol transporter/GFP fusions are targeted to the tonoplast (INT1) or the plasma membrane (INT4) irrespective of the position of the attached GFP (Figures 1B to 1E). We therefore restricted our further analyses to N-terminal GFP fusions. Swapping

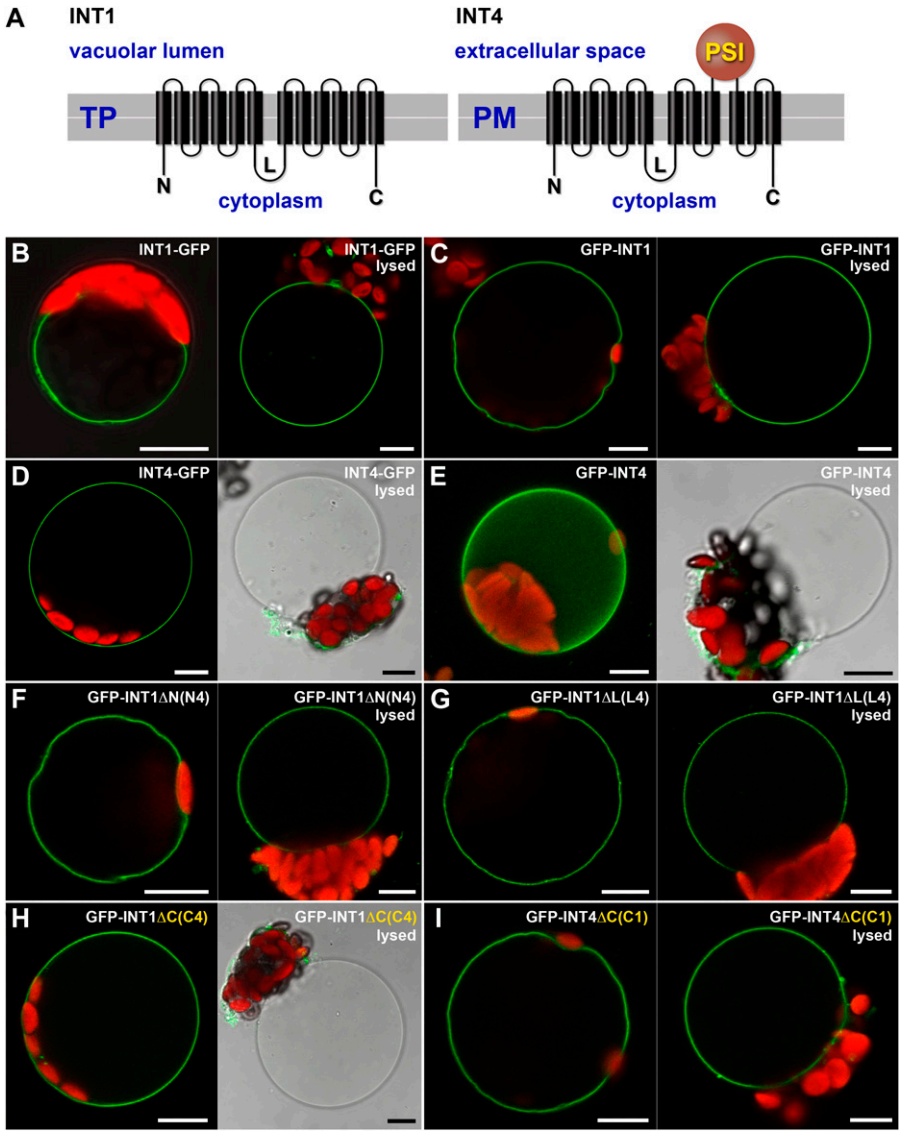

Figure 1. Domain Swapping of N-Terminal, C-Terminal, and Central Loop Sequences between the *Arabidopsis* INT1 and INT4 Proteins.

(A) Schematic drawing showing the position and orientation of INT1 and INT4 in the tonoplast (TP) and the plasma membrane (PM) and the absence or presence of the PSI domain, the most prominent structural difference between the two proteins. N termini (N), C termini (C), and central loops (L) used for domain swapping are indicated.

(B) to **(I)** Confocal images of *Arabidopsis* protoplasts harboring the indicated constructs (left image, intact protoplast; right image, released vacuole after osmotic lysis of the plasma membrane). Red fluorescence shows autofluorescence of chlorophyll. Bars = 10 μm.

(B) to **(E)** Protoplasts transformed with control constructs encoding wild-type INT1 or INT4 proteins with N- or C-terminal GFP.

(F) and **(G)** Domain swapping of the N termini **(F)** or the central loop **(G)** did not affect the subcellular localization.

(H) and **(I)** Domain swapping of the C termini directed the tonoplast transporter INT1 to the plasma membrane **(H)** and the plasma membrane transporter INT4 to the tonoplast **(I)**.

of the N termini (Figure 1F) or exchanging the central loop of INT1 (Figure 1G) did not affect the targeting. Swapping of the C termini, however, rerouted the GFP-INT1ΔC(C4) fusion to the plasma membrane (Figure 1H) and the GFP-INT4ΔC(C1) fusion to the tonoplast (Figure 1I). Identical results were obtained with C-terminal GFP fusions [i.e., with constructs INT1ΔC(C4)-GFP and INT4ΔC (C1)-GFP; see Supplemental Figure 3 online]. This indicated that the C-terminal domains of INT1 and INT4 are required for the targeting of their proteins to the respective membranes.

No rerouting was observed when the C-terminal sequences were added to the intact transporters (i.e., without deletion of the respective other C terminus). The subcellular localization was either almost normal [GFP-INT4(C1)] or the protein was trapped in the ER [GFP-INT4(C1)]. This suggested that the distance of

C-terminal sorting motifs relative to the transmembrane helix might be important (see Supplemental Figure 4 online).

Rerouted INT4 Can Complement the Growth Phenotype of an *int1* Mutant

Having seen that the INT1 C terminus can target the plasma membrane INT4 transporter to the tonoplast, we wanted to know if this rerouted INT4ΔC(C1) protein was intact and functionally active. Although electrochemical proton gradients represent the driving forces both at the tonoplast and at the plasma membrane, different lipid compositions, different sizes of the driving forces, and of course the C-terminal modification in the INT4ΔC (C1) protein might reduce or destroy the transport capacity of the protein. Moreover, a successful complementation would doubtlessly confirm the intactness of the rerouted protein.

Therefore, we expressed the *INT4ΔC(C1)* sequence under the control of the *INT1* promoter (p*INT1*) in an *int1* knockout mutant and tested whether the rerouted INT4ΔC(C1) protein does complement the growth defect of *int1* seedlings on low-inositol medium. Due to a T-DNA insertion in the *INT1* gene, these plants fail to release inositol from their vacuoles during germination, which results in delayed seedling development and poor root growth (Schneider et al., 2008; Figure 2). A direct comparison of seedlings developing from wild-type, *int1*, and *int1/INT4ΔC(C1)* seeds shows that INT4ΔC(C1) fully complements the *int1* phenotype, indicating that this rerouted chimeric protein is functionally active in the tonoplast.

A Di-Leu Motif Targets INT1 to the Tonoplast

For the identification of conserved sequence motifs in the C termini of INT1-type and INT4-type transporters, we assigned characterized or predicted plant inositol transporters to two separate groups based on the presence or absence of plexin-semaphorin-integrin (PSI) domains, and we performed independent alignments of the C-terminal sequences of these proteins (Figure 3). PSI domains were first characterized as extracellular domains of ~100 amino acids in type-I receptors from animal plasma membranes (Bork et al., 1999). Only recently were PSI domains identified in plasma membrane inositol transporters from plants and animals. They are absent from the tonoplast-localized plant paralogs. Removal of the PSI domain neither affected the transport activity nor the sorting to the plasma membrane (Dotzauer et al., 2010).

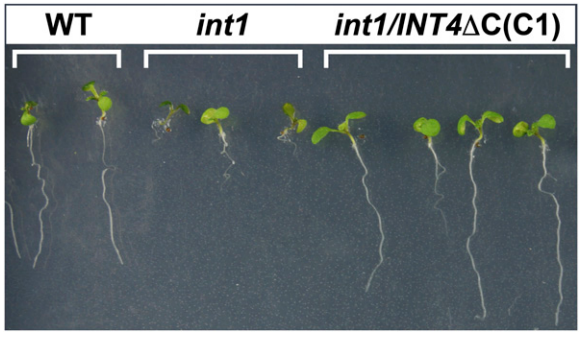

Figure 2. Complementation of the *int1* Phenotype by Tonoplast-Targeted INT4 Protein.

Compared with wild-type *Arabidopsis* plants, *int1* mutants show strongly reduced root development on agar medium with low inositol concentrations. This growth defect is fully rescued in *int1* mutants expressing a fusion construct from the *INT1* promoter that encodes an INT4 protein that has its C terminus replaced by the *INT1* C terminus [*int1/INT4ΔC(C1)* plants]. The image shows seedlings (6 d after germination) on Murashige and Skoog medium supplemented with 2% Suc and 1 mg L^{-1} inositol. WT, wild type.

The alignment of the PSI domain–containing INT transporters (i.e., of characterized and predicted plasma membrane–localized proteins) revealed three conserved sequence motifs in the predicted cytosolic C termini. The first was a [D/E]XXXL[L/I]-type di-Leu motif (Bonifacino and Traub, 2003; EVEKLL in *Arabidopsis* INT4; Figure 3), the second was a conserved [F/Y][K/R] motif (FK in INT4), and the third was characterized by a region of up to five basic amino acids (RRREKK in INT4) and was ~10 amino acids downstream from the di-Leu motif (Figure 3).

The alignment of proteins without PSI domains (i.e., of known or predicted tonoplast transporters) revealed two conserved sequence motifs. The first was a WKERA motif that was almost identical in all INT1-type proteins (Figure 3), and the second was again a [D/E]XXXL[L/I]-type di-Leu motif (NMEGLL in *Arabidopsis* INT1). Although the Leu residues in this motif were more strictly conserved than in the di-Leu motifs of the INT4-type C termini, a typical property of DXXLL sorting motifs (Bonifacino and Traub, 2003), none of the identified di-Leu motifs can be assigned to this second group of di-Leu motifs, as the D in DXXLL motifs is absolutely essential. By contrast, the D or E in [D/E]XXXL[L/I]-type motifs are not well conserved and may be substituted by other, occasionally even basic residues (Bonifacino and Traub, 2003).

We studied the possible role of each of these five sequence motifs on the subcellular localization of INT1 and INT4 by replacing the Leu residues and the adjacent Glu residues (LLE) in INT1 and INT4 by three Ala residues (AAA), by replacing the RRREKK or FK motifs in INT4 by AAAAAA or AA, and by mutating the WKERA sequence of INT1 into WKAAA (Figure 4A). Moreover, we deleted the C-terminal 9 (Δ9) or 30 (Δ30) amino acids of INT1, which removed either the di-Leu motif alone (Δ9) or both conserved motifs (Δ30) from the INT1 C terminus, and we deleted the C-terminal 23 amino acids (Δ23) from the INT4 sequence, which removed all three conserved sequences (Figure 4A). The subcellular localizations of GFP fusions of these modified proteins were studied (Figures 4B to 4J).

The C-terminally deleted INT1 proteins GFP-INT1Δ9 and GFP-INT1Δ30 were no longer targeted to the tonoplast. They rather accumulated in the ER, as shown by the labeling of the ER network in optical sections taken from the top of a protoplast (shown for GFP-INT1Δ30 in Figure 4B) or by the patchy GFP fluorescence in optical sections from the center of a protoplast (shown for GFP-INT1Δ9 in Figure 4C). No fluorescence of the tonoplast was obtained with these constructs after lysis of the plasma membrane (Figure 4C, right image). Mutations in the WKERA motif of INT1 (Figure 4D) did not affect the subcellular targeting of the modified proteins. Interestingly, however,

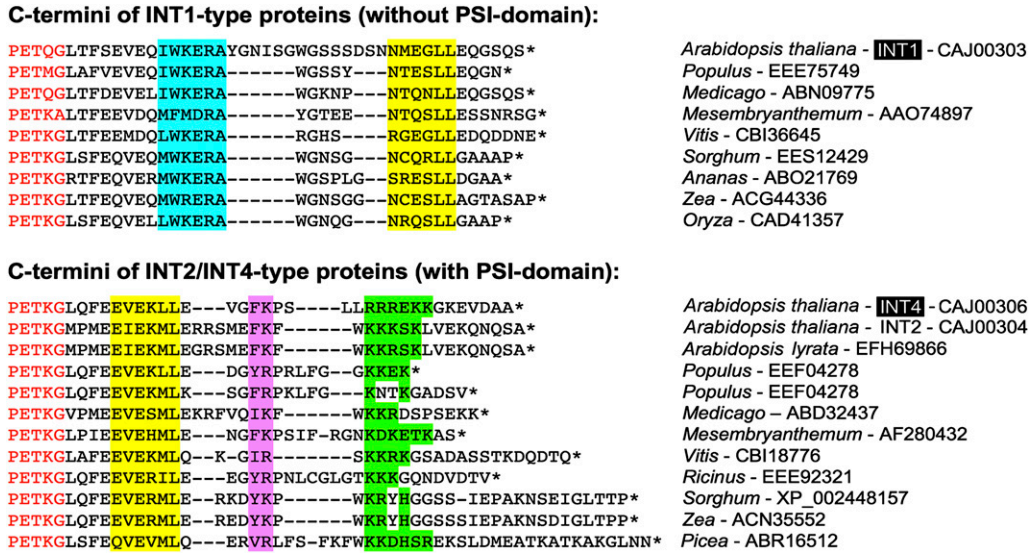

Figure 3. Alignment of the C-Terminal Sequences from INT1-Type and INT4-Type Transporters.

Sequences obtained from BLAST analyses (http://www.ncbi.nlm.nih.gov/blast/Blast.cgi) were divided into two groups based on the presence or absence of a PSI domain between their predicted transmembrane helices IX and X and listed as INT1-type transporters **(Top)** or as INT4-type transporters **(Bottom)**. A consensus sequence at the start of the C terminus of plant and animal transporters of the major facilitator superfamily (Marger and Saier, 1993) is shown in red. Di-Leu motifs are highlighted in yellow, a conserved region found only in INT1-type transporters is highlighted in blue, and conserved regions found only in INT4-type transporters are highlighted in magenta and green. Gene names or genus names plus GenBank accession numbers are given.

replacement of the di-Leu motif in the INT1 C terminus by Ala residues resulted in a complete loss of GFP fluorescence in the tonoplast (Figure 4E) and in an efficient and complete targeting of the GFP-INT1$_{(LLE \rightarrow AAA)}$ protein to the plasma membrane. No labeling of the ER network was detected in protoplasts expressing the *GFP-INT1$_{(LLE \rightarrow AAA)}$* construct as shown by the maximum projection in Figure 4E. The identical result was obtained with a *GFP-INT1$_{(LLE \rightarrow SSS)}$* construct (see Supplemental Figure 5 online).

Unexpectedly, neither the mutations in the conserved INT4 motifs (Figures 4F to 4I) nor the deletion of the 23 C-terminal amino acids of INT4 (Figure 4J) had any effect on the targeting of the INT4 protein to the plasma membrane. This was confirmed by colocalization analyses of GFP-INT4$_{(LLE \rightarrow AAA)}$ and of unmodified INT4-RFP (Figure 4H) and by the maximum projections shown in Figures 4I and 4J. As in Figures 1E and 4E, these projections show a uniformly labeled cell surface and no fluorescence of the subjacent ER. Together, these results (1) demonstrated that of the five motifs analyzed, only the di-Leu motif in the INT1 C terminus is critical for the correct targeting, and (2) they suggested that presumably no sorting sequence is present in the INT4 C terminus.

The INT1 C Terminus Can Redirect Other Transporters to the Tonoplast

As the intact INT1 C terminus is required for the targeting of INT1 or the closely related INT4 protein to the tonoplast, it might also be a useful tool to modify the subcellular localization of less closely related transporters. To test this hypothesis, we fused the INT1 C terminus to the well-characterized *Arabidopsis* Suc transporter SUC2, a plasma membrane protein with 12 transmembrane helices (Sauer and Stolz, 1994; Truernit and Sauer, 1995; Stadler and Sauer, 1996), and to the recently published SWEET1 protein, a monosaccharide facilitator with seven transmembrane helices reported to reside primarily in the plasma membrane (Chen et al., 2010). The C termini of both proteins are predicted to face the cytoplasm (i.e., to have the same topological orientation as the INT1 C terminus).

Fusions between SUC2 and the INT1 C terminus were generated either with the intact SUC2 transporter or with a SUC2 protein that had 14 amino acids of its C terminus deleted (Δ14) (i.e., all except two amino acids after the 12th transmembrane helix). Figures 5A and 5B show that the GFP-SUC2 and SUC2-GFP controls labeled the plasma membrane as expected. Addition of the INT1 C terminus to the intact SUC2 protein had no effect on this subcellular localization both with N-terminal (Figure 5C) or C-terminal GFP (Figure 5D). Moreover, C-terminally deleted SUC2 constructs were also sorted to the plasma membrane irrespective of the position of GFP (Figures 5E and 5F), indicating that the SUC2 C terminus is not required for protein sorting to the plasma membrane. Replacement of the 14 C-terminal amino acids of SUC2 by the INT1 C terminus, however, directed both GFP-SUC2Δ14(C1) (Figure 5G) and SUC2Δ14(C1)-GFP (Figure 5H) to the tonoplast, although to a different extent (see Supplemental Table 1 online). Whereas GFP-SUC2Δ14(C1) was targeted exclusively to the tonoplast (Figure 5G), only weak labeling of the tonoplast was observed with SUC2Δ14(C1)-GFP, which was still sorted to the plasma membrane to a large extent (Figure 5H). The results obtained in

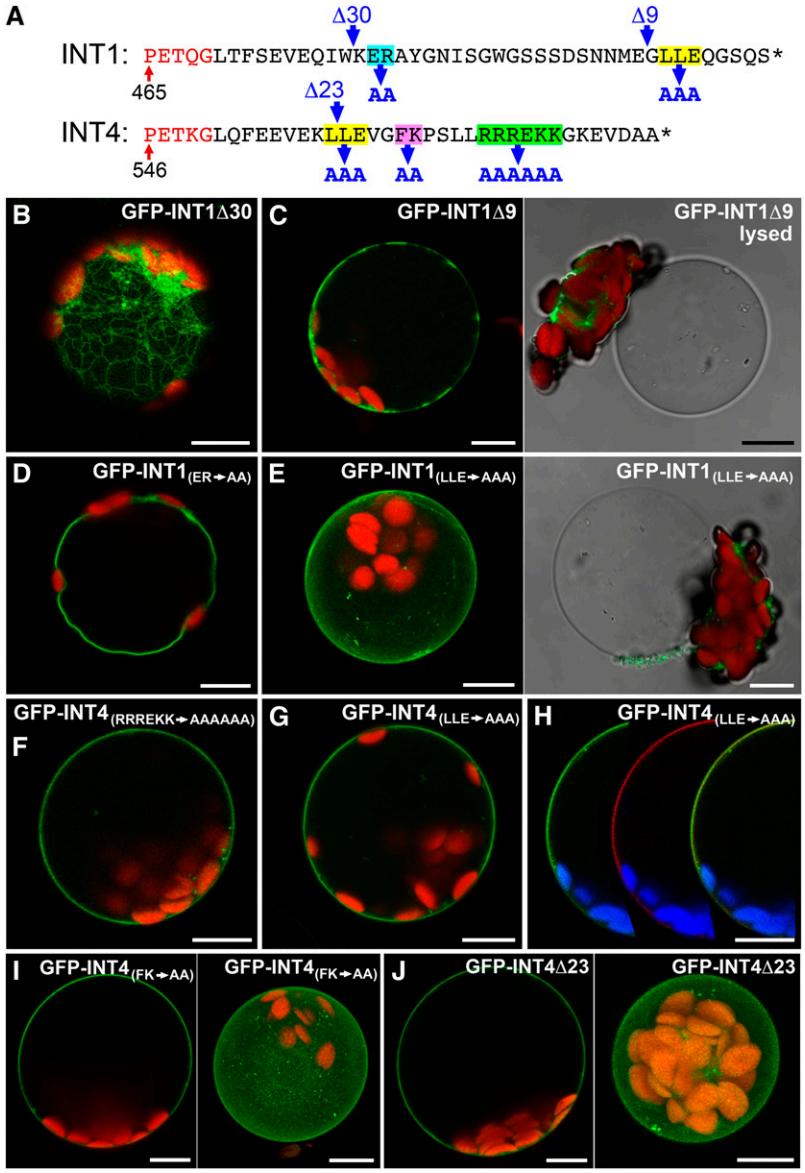

Figure 4. Deletions and Mutational Analyses of INT1 and INT4 C Termini.

(A) C-terminal sequences starting with a sequence motif (red) conserved at the start of the C termini of all MST-like family members. The position of the Pro residues in INT1 or INT4 is given. The di-Leu motifs conserved in INT1-type and INT4-type transporters are highlighted in yellow and sequence motifs conserved only in INT1-type or in INT4-type transporters in blue, magenta, or green. Deletions and mutations are shown in blue.
(B) to **(J)** Confocal images. Chlorophyll autofluorescence is shown in red in **(B)** to **(G)**, **(I)**, and **(J)** or in blue in **(H)**. Bars = 10 μm.
(B) The INT1Δ30 deletion construct is trapped in the ER as indicated by the fluorescent ER network in a section taken near the top of a protoplast.
(C) The INT1Δ9 deletion construct is also trapped in the ER as indicated by the patchy fluorescence in the section from the center of a protoplast. No fluorescence was detected in the tonoplast after lysis of the plasma membrane.
(D) Replacing the Glu and Arg residues in the conserved WKERA motif by two Ala residues did not affect the targeting of INT1 to the tonoplast.
(E) Replacing the di-Leu motif by three Ala residues resulted in a complete loss of tonoplast fluorescence (right). The modified INT1 protein was rather guided to the plasma membrane. The maximum projection (left) shows no labeling of the ER.
(F) The GFP-INT4$_{(RRREKK \rightarrow AAAAAA)}$ mutation in the INT4 C terminus did not affect the targeting of the modified protein to the plasma membrane.
(G) Similarly, the GFP-INT4$_{(LLE \rightarrow AAA)}$ mutation did not affect the targeting.
(H) Plasma membrane localization of GFP-INT4$_{(LLE \rightarrow AAA)}$ was confirmed by cotransformation of an *INT4-RFP* construct, independent detection of the GFP (left) and RFP (center) signals, and merging of the images (right).
(I) The GFP-INT4$_{(FK \rightarrow AA)}$ mutation did not affect the targeting (left, optical section; right, maximum projection).
(J) Deletion of 23 C-terminal amino acids did not affect the targeting (left, optical section; right, maximum projection).

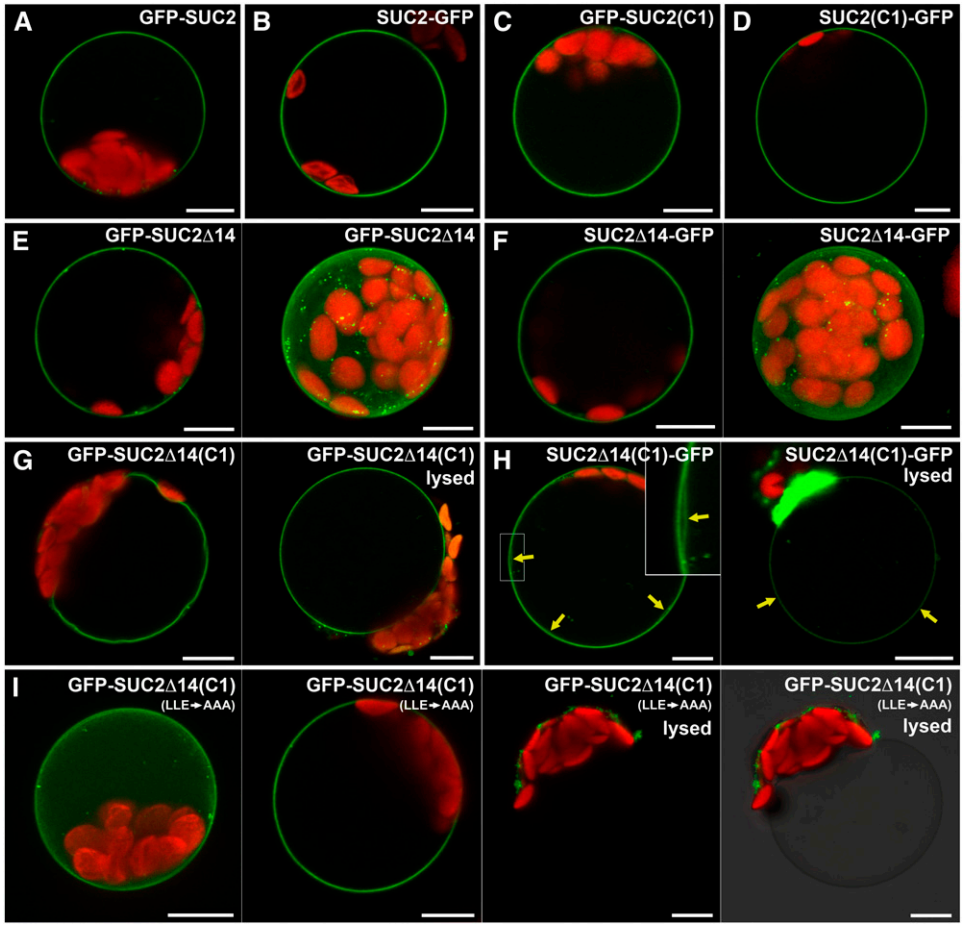

Figure 5. Targeting of SUC2 to the Tonoplast.

Single optical sections (**[A]** to **[D]**, **[G]**, **[H]**, left images in **[E]** and **[F]**, and all images but the first in **[I]**) or maximum projections (right images in **[E]** and **[F]**, left image in **[I]**) are shown. Red color shows chlorophyll autofluorescence in all images. Bars = 10 μm.

(A) A GFP-SUC2 fusion labels the plasma membrane.

(B) A SUC2-GFP fusion labels the plasma membrane.

(C) Addition of the INT1 C terminus does not affect sorting of GFP-SUC2(C1) to the plasma membrane.

(D) Addition of the INT1 C terminus does not affect sorting of SUC2(C1)-GFP to the plasma membrane.

(E) Deletion of 14 C-terminal amino acids does not affect sorting to the plasma membrane of a GFP-SUC2Δ14 fusion.

(F) Deletion of 14 C-terminal amino acids does not affect sorting to the plasma membrane of a SUC2Δ14-GFP fusion.

(G) Replacement of the 14 C-terminal amino acids by the INT1 C terminus results in perfect sorting to the tonoplast of GFP-SUC2Δ14(C1) in intact protoplasts (left) and after osmotic lysis of the plasma membrane (right).

(H) SUC2Δ14(C1)-GFP is less efficiently sorted to the tonoplast than GFP-SUC2Δ14(C1) (see **[G]** for comparison). In addition to the plasma membrane, labeling of the tonoplast is seen both in intact protoplasts (yellow arrows in left image; inset shows the boxed region at higher magnification) and in vacuoles after osmotic lysis of the plasma membrane.

(I) The GFP-SUC2Δ14(C1)$_{(LLE \rightarrow AAA)}$ mutation abolishes targeting of SUC2 to the tonoplast by the INT1 C terminus as indicated by the fluorescence images of a lysed protoplast (right images, plus and minus white light image). It rather results in a uniform labeling of the plasma membrane (left images, maximum projection and optical section of intact protoplasts).

Figures 4B to 4E suggested that the di-Leu motif in the INT1 C terminus is required for tonoplast sorting. When we introduced the LLE→AAA mutation studied in Figure 4E into the C terminus of the GFP-SUC2Δ14(C1) protein, the resulting GFP-SUC2Δ14 (C1)$_{(LLE \rightarrow AAA)}$ protein was no longer sorted to the tonoplast but rather targeted exclusively to the plasma membrane (Figure 5I), confirming that di-Leu is required for tonoplast sorting. Moreover, this result demonstrated again that removal of a specific sorting signal resulted in targeting to the plasma membrane.

Fusions between SWEET1 and the INT1 C terminus were made either with the intact SWEET1 transporter or with a SWEET1 protein that had 33 amino acids of its C terminus deleted (Δ33) (i.e., most of its 38–amino acid cytoplasmic tail).

Figures 6A and 6C show that in contrast with the published SWEET1 localization in the plasma membrane (Chen et al., 2010), the GFP-SWEET1 and SWEET1-GFP controls labeled primarily the ER. However, an additional almost negligible staining in the plasma membrane was observed in few protoplasts expressing *SWEET1-GFP*. The same result was obtained 72 h after transformation of protoplasts, indicating that the localization of SWEET1 in the ER was not only transient due to a slower trafficking rate (see Supplemental Figure 6 and Supplemental Table 1 online). However, in line with the published data, tonoplast fluorescence was observed with none of these constructs (Figures 6A and 6C). Moreover, C-terminally deleted GFP-SWEET1Δ33 was also sorted exclusively to the ER (Figure 6B). As with SUC2, addition of the INT1 C terminus to the intact transporter had no effect on the subcellular localization, and GFP-SWEET1(C1) labeled the ER (Figure 6D) just as the unmodified or C-terminally deleted SWEET1 protein (Figures 6A to 6C). Replacement of the 33 C-terminal amino acids by the INT1 C terminus, however, directed the resulting GFP-SWEETΔ33(C1) protein to the tonoplast (Figure 6E).

AP-3 Is Involved in the Sorting of SUC4 to the Tonoplast but Is Not Involved in INT1 Sorting

It has been suggested in several publications that the AP-3 adapter complex from *Arabidopsis* is involved in protein sorting to the vacuole (Sanmartín et al., 2007; Sohn et al., 2007; Feraru et al., 2010; Zwiewka et al., 2011). Moreover, phylogenetic analyses indicate that, in fact, the β-subunit (At3g55480) of this *Arabidopsis* complex is most closely related to the β-subunits of the yeast and human AP-3 complexes (see Supplemental Figure 7 and Supplemental Data Set 1 online), which are involved in sorting to the lysosome and are known to recognize [D/E]XXXL[L/I]-type sorting signals (Bonifacino and Traub, 2003). To test if AP-3 is also involved in tonoplast sorting of INT1, we expressed a *GFP-INT1* fusion construct both in *AP-3* wild-type plants and in a mutant line defective in the β-subunit of the AP-3 complex (*ap-3* β mutant). This mutant line (SAIL_1258_G03) is identical with the previously published *pat2-2* (for *protein affected trafficking2-2*) mutant (Feraru et al., 2010).

Figures 7A and 7B demonstrate that the *ap-3* β mutation does not affect INT1 sorting, as wild-type and *ap-3* β mutant protoplasts

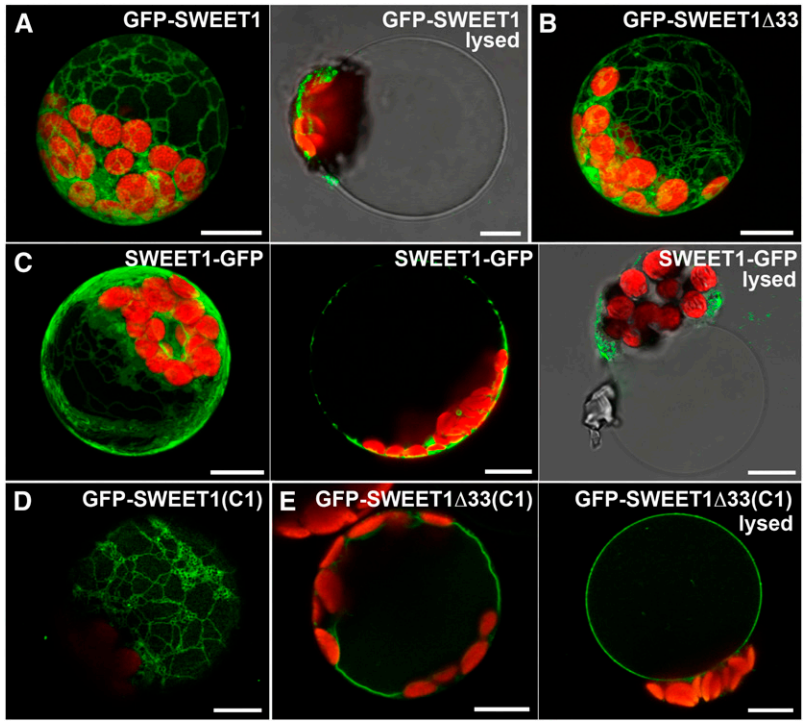

Figure 6. Targeting of SWEET1 to the Tonoplast.

(A) Wild-type SWEET1 with GFP at its N terminus is targeted exclusively to the ER (left; maximum projection) and does not label the tonoplast (right; optical section).
(B) Deletion of 33 C-terminal amino acids does not affect this localization (maximum projection).
(C) Wild-type SWEET1 with GFP at its C terminus is also targeted to the ER network (in some protoplasts, additional weak labeling of the plasma membrane was observed [left; maximum projection]). Optical section through a protoplast expressing the *SWEET1-GFP* construct showing patchy fluorescence, which is in line with labeling of the ER (center). SWEET1-GFP never labels the tonoplast (right; optical section).
(D) Addition of the INT1 C terminus to the intact SWEET1 protein also does not affect this localization (maximum projection).
(E) Replacement of the 33 C-terminal amino acids by the INT1 C terminus results in labeling of the tonoplast in intact protoplasts (left; optical section) and after osmotic lysis of the plasma membrane (right; optical section).
Red color shows chlorophyll autofluorescence. Bars = 10 μm.

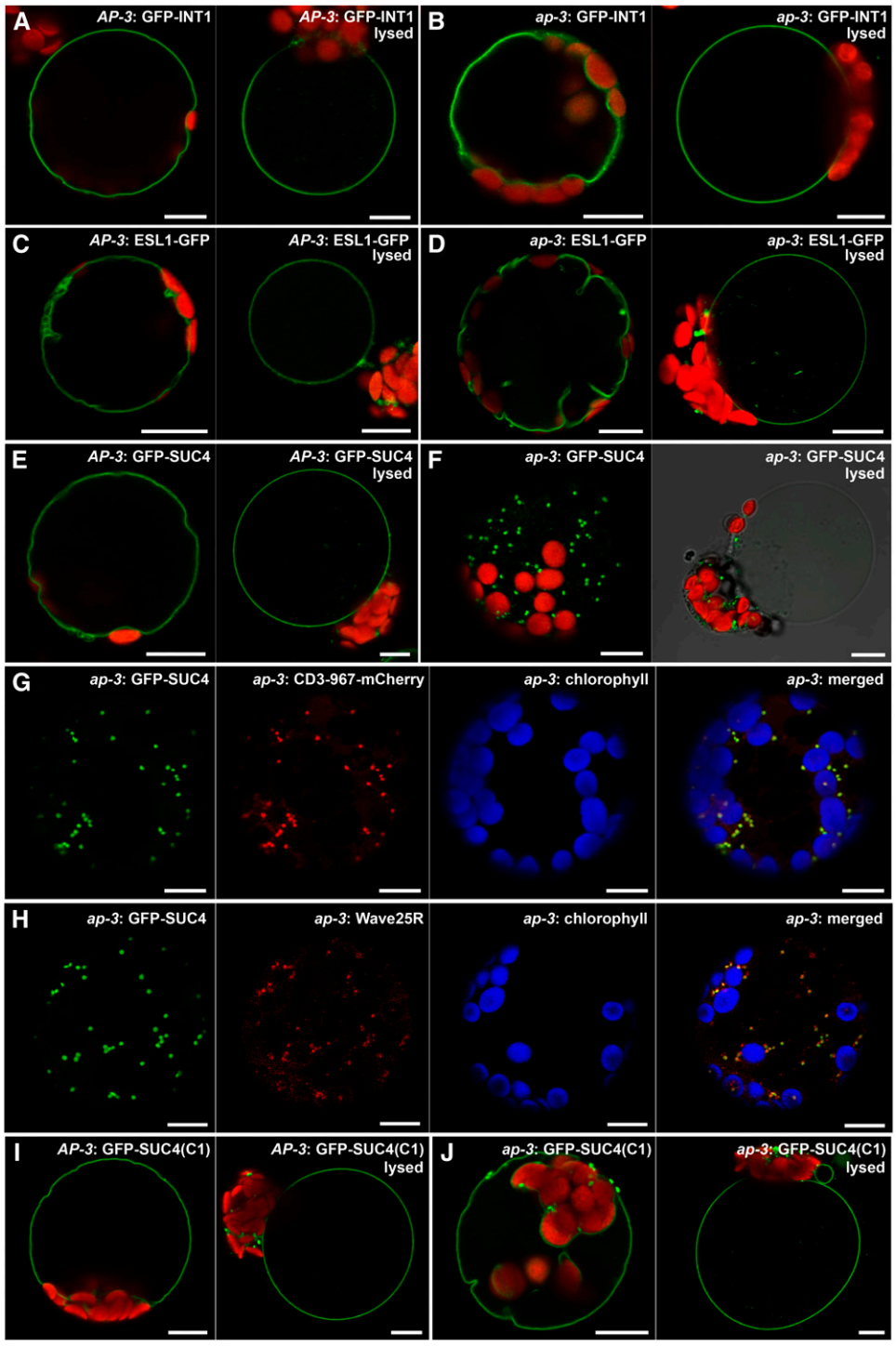

Figure 7. The AP-3 Complex Targets SUC4 to the Tonoplast but Does Not Target the Di-Leu Motif–Containing INT1 and ESL1 Transporters.

All images are single optical sections and show intact protoplasts (left images in **[A]** to **[F]**, **[I]**, **[J]**, and all images in **[G]** and **[H]**) or vacuoles after osmotic lysis of the plasma membrane (right image in **[A]** to **[F]**, **[I]**, and **[J]**). **(A)**, **(C)**, **(E)**, and **(I)** show analyses in protoplasts obtained from *AP-3* wild-type plants. **(B)**, **(D)**, **(F)**, **(G)**, **(H)**, and **(J)** show analyses in protoplasts obtained from *ap-3* mutants. Red color in **(A)** to **(F)**, **(H)**, and **(I)** shows chlorophyll autofluorescence. Bars = 10 μm.

(A) and **(B)** GFP-INT1 is targeted to the tonoplast in *AP-3* wild-type and *ap-3* mutant plants.

(C) and **(D)** ESL1-GFP is targeted to the tonoplast in *AP-3* wild-type and *ap-3* mutant plants.

show the same and exclusive localization of GFP-INT1 to the tonoplast. As controls, we compared the localization of GFP fusions to the *Arabidopsis* Suc transporter SUC4 (GFP-SUC4) and to the *Arabidopsis* Glc transporter ESL1 (ESL1-GFP), which were previously shown to localize to the tonoplast (Endler et al., 2006; Yamada et al., 2010; Schneider et al., 2011). Whereas ESL1 has an N-terminal [D/E]XXXL[L/I]-type motif involved in the sorting to the tonoplast (Yamada et al., 2010), SUC4 does not contain any of the putative sorting signals known from animals. In line with the published data, ESL1-GFP and GFP-SUC4 constructs labeled exclusively the tonoplast of *AP-3* wild-type plants (Figures 7C and 7E). Moreover, as already seen for the GFP-INT1 fusion, the sorting of ESL1-GFP was not affected by the *ap-3* mutation (Figure 7D). Surprisingly, however, sorting of GFP-SUC4 to the tonoplast was blocked completely in the *ap-3* β mutant and resulted in the labeling of punctate structures (Figure 7F).

INT1 and SUC4 Are Sorted to the Tonoplast via Two Different Golgi-Dependent Routes

Cotransformation of *ap-3* β protoplasts with constructs for GFP-SUC4 and the soybean (*Glycine max*) α-1,2-mannosidase I–derived *cis*-Golgi marker CD3-967-mCherry (Saint-Jore-Dupas et al., 2006; Nelson et al., 2007) suggested that the punctate structures seen in Figure 7F might show accumulation of GFP-SUC4 in the *cis*-Golgi (Figure 7G). In fact, cotransformation of *ap-3* β protoplasts with constructs for GFP-SUC4 and another *cis*-Golgi marker, the *Arabidopsis* v-SNARE MEMBRIN12 (MEMB12) (Uemura et al., 2004), which carries an mCherry-fusion in the Wave127R construct published by Geldner et al. (2009), showed the same colocalization (see Supplemental Figure 8A online). Moreover, at higher magnifications, the labeled structures were clearly donut shaped, which is typical for Golgi stacks but not for the TGN (see Supplemental Figure 8B online; Langhans et al., 2007). Finally, when we coexpressed *GFP-SUC4* with the Wave25R construct (Geldner et al., 2009), which harbors the Golgi and TGN-localized GTPase RabD1 (Pinheiro et al., 2009), we observed red fluorescence mostly in the immediate vicinity of the green fluorescent, GFP-SUC4–labeled Golgi (see Supplemental Figure 9 online). This confirmed that GFP-SUC4 does not accumulate in the TGN of *ap-3* β mutants.

It is well established that targeting of the aquaporin α-TIP to protein storage vacuoles (PSVs) occurs Golgi independently (Jiang and Rogers, 1998; Park et al., 2004), and only recently, it was also shown that in rice, the two-pore K^+ channel TPKb is sorted to PSVs in a Golgi-independent manner directly from the ER (Isayenkov et al., 2011). This model was based on the observation that this sorting was not affected by the fungal antibiotic brefeldin A (BFA), which interferes with protein transport from the ER to the Golgi by disrupting Golgi membrane integrity (Nebenführ et al., 2002). In parallel analyses, sorting of the second two-pore K^+ channel from rice, TPKa, to lytic vacuoles (LVs) was inhibited by BFA (Isayenkov et al., 2011).

The *Arabidopsis* mesophyll protoplasts studied in this article contain only a single central vacuole representing a typical LV (Marty, 1999). We compared the effect of 25 μg mL^{-1} BFA on the sorting of GFP-INT1 and GFP-SUC4 to the tonoplast according to the protocol described by Isayenkov et al. (2011). The plasma membrane–localized GFP-INT4 fusion was included as a control. Figures 8A to 8C show that all three fusion constructs are sorted to the correct membrane in the presence of 0.25% DMSO, the solvent used to prepare the BFA stock solution. Figures 8D to 8F demonstrate that protoplasts coexpressing the different GFP fusions with the *cis*-Golgi marker CD3-967-mCherry accumulate all proteins in a vesicular ER. Most importantly, these protoplasts contain an intact vacuole (yellow arrows in Figures 8E and 8F; for a colocalization image of GFP-SUC4 and CD3-967-mCherry in the absence of BFA and for an image of a BFA-treated protoplast expressing *GFP-SUC4* only, see Supplemental Figure 10 online). Furthermore, BFA treatment did not affect protoplast viability, since 6 h after BFA removal the original subcellular localization of INT4, INT1, and SUC4 was reestablished (see Supplemental Figure 11 online).

In summary, these data demonstrate (1) that *Arabidopsis* possesses two alternative routes for the sorting of INT1 and SUC4 to the central vacuole; (2) that SUC4 is sorted via an AP-3–dependent route, whereas sorting of INT1 is AP-3-independent; (3) that blocking the AP-3 route leads to accumulation of GFP-SUC4 in the Golgi and not in the TGN; and (4) that both sorting routes involve the Golgi.

Based on all these data, we finally speculated that, if SUC4 and INT1 are sorted to the tonoplast via different routes and if the identified C-terminal sorting signal of INT1 (Figures 4 to 6; see Supplemental Figure 5 online) is required for sorting via the AP-3–independent route, it should be possible to bypass the block of GFP-SUC4 sorting in the *ap-3* β mutant and to sort GFP-SUC4 to the tonoplast via the INT1 route by adding the INT1 C terminus to SUC4. This is, in fact, the case. Figures 7I and 7J show that the fluorescent GFP-SUC4(C1) chimera is targeted to the tonoplast not only in *AP-3* β wild-type protoplasts (Figure 7I) but also in protoplasts of the *ap-3* β mutant (Figure 7J).

DISCUSSION

In this study, we demonstrate that a di-Leu motif in the C terminus of the tonoplast-localized inositol transporter INT1 is indispensable

Figure 7. (continued).

(E) and **(F)** GFP-SUC4 is targeted to the tonoplast in *AP-3* wild-type plants but trapped in the Golgi of *ap-3* mutants.

(G) Protoplast of an *ap-3* mesophyll cell cotransformed with constructs for GFP-SUC4 (left) and the *cis*-Golgi marker CD3-967-mCherry (second from left). A merge of these images (right) and of an image of the chlorophyll autofluorescence (blue; third image from left) shows that GFP-SUC4 is trapped in the Golgi.

(H) Protoplast of an *ap-3* mesophyll cell cotransformed with constructs for GFP-SUC4 (left) and the Golgi/TGN marker Wave25R-mCherry (second from left). A merge of these images (right) and of an image of the chlorophyll autofluorescence (blue; third image from left) shows that GFP-SUC4 is trapped in the Golgi.

(I) and **(J)** GFP-SUC4(C1) is targeted to the tonoplast in *AP-3* wild-type and *ap-3* mutant plants.

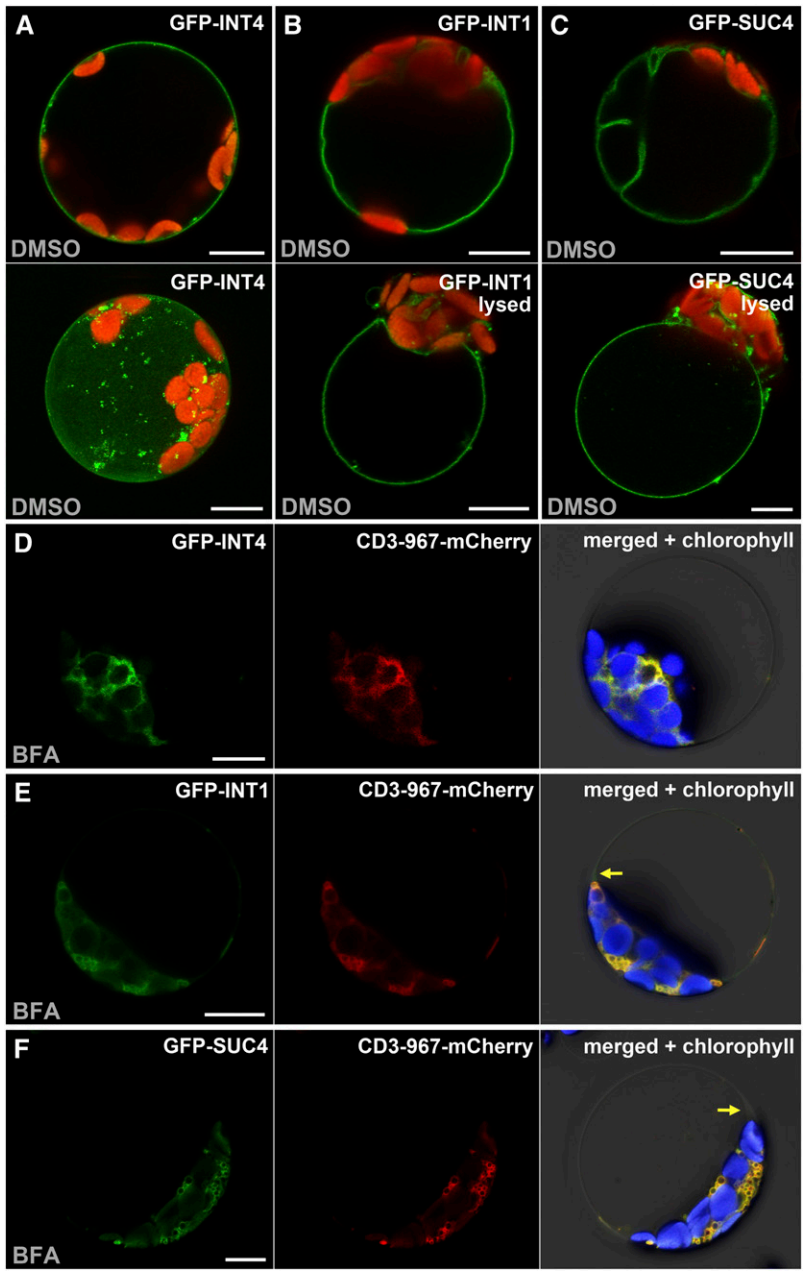

Figure 8. BFA Sensitivity of INT4, INT1, and SUC4 Sorting in Mesophyll Protoplasts from Wild-Type Plants.

(A) to **(C)** are controls treated with 0.25% DMSO only (chlorophyll autofluorescence shown in red), and **(D)** to **(F)** show the effects of BFA treatment (25 μg mL^{-1}) in the presence of 0.25% DMSO (chlorophyll autofluorescence shown in blue). The bottom image in **(A)** shows a maximum projection; all other images are optical sections. All localizations were studied in at least 40 to 50 protoplasts, which all showed the identical localizations. Yellow arrows in **(E)** and **(F)** show the presence of intact vacuoles after the BFA treatment. Bars = 10 μm.

(A) Protoplast expressing *GFP-INT4*.

(B) Intact **(Top)** and lysed protoplasts **(Bottom)** expressing *GFP-INT1*.

(C) Intact **(Top)** and lysed protoplasts **(Bottom)** expressing *GFP-SUC4*.

(D) Protoplast coexpressing *GFP-INT4* (left) and *CD3-967-mCherry* (middle) in the presence of BFA. The right image shows a merge of the green and red channels plus chloroplast autofluorescence.

(E) Protoplast coexpressing *GFP-INT1* (left) and *CD3-967-mCherry* (middle) in the presence of BFA. The right image shows a merge of the green and red channels plus chloroplast autofluorescence.

(F) Protoplast coexpressing *GFP-SUC4* (left) and *CD3-967-mCherry* (middle) in the presence of BFA. The right image shows a merge of the green and red channels plus chloroplast autofluorescence.

for correct targeting of INT1 to the tonoplast. Moreover, we showed that plasma membrane– and ER-localized transporters can be redirected to the tonoplast via the INT1 C terminus. These data are relevant for the molecular breeding of plants with altered storage properties in their vacuoles, as they provide a simple tool to redirect transporters with known transport functions to the central vacuole, the major storage compartment of higher plants.

We also demonstrate that the C terminus of INT1 mediates an AP-3–independent trafficking pathway, similar as it was shown for tonoplast sorting of ESL1 (Yamada et al., 2010). By contrast, another tonoplast-localized transporter, the Suc transporter SUC4 (Endler et al., 2006; Schneider et al., 2011; Schulz et al., 2011), is transported via a second, AP-3–dependent route.

A C-Terminal Di-Leu Motif Is Involved in INT1 Sorting to the Tonoplast

The identified di-Leu motif in the INT1 C terminus (NMEGLL) belongs to the group of acidic [D/E]XXXL[L/I] sorting motifs previously characterized in mammals and yeast (Bonifacino and Traub, 2003). Although acidic residues are frequently observed at position −4 from the first Leu, which led to the name of the motif, these residues are important only in few proteins and may be replaced in most others (Letourneur and Klausner, 1992; Bonifacino and Traub, 2003). For example, a [D/E]XXXL[L/I]-type sorting motif identified in the C terminus of the Glc facilitator GLUT4 from humans (RTPSLLEQ; Sandoval et al., 2000) is quite similar to that of INT1 (NMEGLLEQ) but has a basic residue at the −4 position. The sorting motif in the INT1 C terminus clearly does not belong to the DXXLL group of sorting signals, a distinct type of di-Leu motifs frequently found in animals. In DXXLL signals, the requirement for the D and LL residues is quite strict (Bonifacino and Traub, 2003), and mostly these signals are separated only by one or two residues from the C termini of the proteins.

Our results demonstrate that the INT1 C terminus is required for the tonoplast sorting of INT1 and several fusion proteins. For most chimera, the C terminus of the protein in question had to be replaced by the INT1 C terminus for a successful sorting to the tonoplast. A simple addition of the INT1 C terminus to intact INT4, SUC2, or SWEET1 had no recognizable effect, suggesting that the distance relative to the transmembrane helix is important for successful sorting. An exception was the SUC4(C1) chimera that was sorted to the tonoplast without deletion of the SUC4 C terminus. This quite likely is due to the short SUC4 C terminus, which is only 10 amino acids. In fact, critical distances were described for most sorting motifs in animals (Geisler et al., 1998; Bonifacino and Traub, 2003).

The Absence of a Functional Sorting Signal Drives Proteins to the Plasma Membrane

Secretion is known to be the default destination in plant cells for soluble proteins lacking sorting signals within the secretory pathway (Chrispeels, 1991; Bednarek and Raikhel, 1992), but the default membrane is unclear. The observation that several of our mutated or chimeric proteins were sorted to the plasma membrane might indicate that the plasma membrane is the default membrane in the absence of specific sorting signals. However, type-I membrane proteins without a specific sorting signal were previously shown to accumulate in different membranes (ER, Golgi, or plasma membrane) depending on the length of their single transmembrane helix (Brandizzi et al., 2002). None of the proteins was sorted to the tonoplast. Other data, which were obtained with partial α-TIP sequences (Höfte and Chrispeels, 1992; Jiang and Rogers, 1998), suggested that the tonoplast might be the default membrane.

One might argue that the plasma membrane sorting of INT4 (C1) and SUC2(C1) chimera that had their own C termini not removed might not only be caused by the wrong distance between the INT1 di-Leu motif and the last transmembrane helix. In addition, endogenous sorting motifs in the INT4 and SUC2 C termini might direct these proteins to the plasma membrane. However, neither the mutations in the INT4 C terminus nor the deletion of the entire INT4 or SUC2 C termini affected the subcellular sorting of the modified proteins, suggesting that specific plasma membrane sorting signals are not present in these C termini. In fact, di-Leu–type or Tyr-based sorting motifs were not found in the C terminus of the SUC2 protein.

Most importantly, however, mutations in the di-Leu motif in the INT1 C terminus (LLE→AAA and LLE→SSS) caused a complete shift of the mutated proteins from the tonoplast to the plasma membrane, indicating that the removal of the tonoplast-sorting motif is sufficient to sort INT1 to the plasma membrane. Finally, the same LLE→AAA mutation in the GFP-SUC2Δ14(C1) fusion abrogated the artificially engineered tonoplast localization of this protein and directed this protein back to the plasma membrane.

Together, these data suggest that the analyzed proteins are targeted to the plasma membrane due to the absence of a specific sorting signal and that the plasma membrane is the default membrane in plants. In line with this model, a mutation in the N-terminal di-Leu motif of the tonoplast-localized ESL1 transporter was shown to cause sorting of this protein to the plasma membrane of *Arabidopsis* guard cells and of tobacco (*Nicotiana tabacum*) BY-2 suspension cells (Yamada et al., 2010).

Interestingly, C-terminally truncated INT1Δ9 and INT1Δ30 proteins were trapped in the ER and did not accumulate in the plasma membrane as the di-Leu motif–deficient GFP-$INT1_{(LLE\rightarrow AAA)}$ and GFP-$INT1_{(LLE\rightarrow SSS)}$ proteins. This might indicate that either the INT1 C terminus is also required for the exit from the ER, a function that is obviously not affected by the LLE→AAA mutation, or that these mutated proteins are not properly folded and therefore remain in the ER.

Transporters Are Sorted to the Tonoplast via Different Routes

It is widely accepted that plant cells contain different types of vacuoles, such as LVs and PSVs. Both types of vacuoles can even coexist in the same cell (e.g., in the root tips of seedlings; Paris et al., 1996). Therefore, in these cells, two targeting mechanisms must exist to allow specific sorting of membrane proteins to LVs and PSVs.

Based on the observation that targeting of α-TIP and soluble phytohemagglutinin was differently affected by inhibitors of protein transport, it has been proposed that soluble and

membrane proteins reach the vacuole by different paths (Gomez and Chrispeels, 1993). A few years later, two different sorting mechanisms for α-TIP and γ-TIP were reported (Jiang and Rogers, 1998), indicating distinct routes for the sorting of membrane proteins to vacuoles. In these analyses, fusions of C-terminal regions from α-TIP and γ-TIP to the single transmembrane helix of the sorting receptor BP-80 either retained the normal targeting of BP-80 to lytic PVCs (C terminus of γ-TIP) or not (C terminus of α-TIP). Recent analyses on the sorting of the rice two-pore K^+ channels TPKa (sorted to LVs) and TPKb (sorted to PSVs) again suggested the existence of different pathways (Isayenkov et al., 2011). TPKb appeared to be sorted via a Golgi-independent and BFA-insensitive pathway, but sorting of TPKa was dependent on an intact Golgi system and sensitive to BFA. Truncations and mutational analyses of the C termini suggested that these parts of TPKa and TPKb determine the sorting to LVs or PSVs. However, specific sequence motifs were not identified. Analyses of the putative sorting function of N-terminal [D/E]XXXL[L/I]-type sorting motifs conserved in TPKa and TPKb and also in the LV-localized *Arabidopsis* homolog TPK1 (Dunkel et al., 2008) were not included.

In contrast with these analyses, our studies did not compare the sorting to LVs and PSVs. Moreover, the model of multivacuoles is rather exceptional and does only apply for specific cells (Frigerio et al., 2008).The two different routes identified for INT1 and SUC4 both target their cargo proteins to the large central vacuole of *Arabidopsis* mesophyll cells. Although *Arabidopsis* AP-3 β had so far not been shown to be directly involved in the sorting of a specific cargo protein, the identification of AP-3 β as a component of a vacuolar sorting route is not unexpected, as important roles of different AP-3 subunits for vacuolar function and biogenesis have been described (Feraru et al., 2010; Zwiewka et al., 2011). Moreover, the AP-3 complex from bakers' yeast was identified and characterized after the observation that sorting of the type-II integral vacuolar membrane protein alkaline phosphatase was not affected by mutations in genes involved in the classical vacuolar sorting route via the PVC (Cowles et al., 1997a, 1997b). In fact, AP-3 in yeast appears to transport its cargo proteins directly from the Golgi to the vacuole bypassing the PVC (Odorizzi et al., 1998; Dell'Angelica, 2009).

In the fruit fly *Drosophila melanogaster*, mutations in the AP-3 δ-subunit lead to eye color mutations, as the normal development of lysosome-related pigment granules is disturbed (Lloyd et al., 1998). Similarly, in mice and humans, mutations in the AP-3 β- or δ-subunits result in color mutations and a special form of albinism, the Hermansky-Pudlak syndrome, which is a consequence of the abnormal formation of lysosome-related melanosomes (Dell'Angelica et al., 1999). In contrast with yeast, animal AP-3 recruits its cargo on early endosomes for the sorting to lysosomes or lysosome-related organelles; however, the possibility of cargo recruitment already at the Golgi is still being discussed (Dell'Angelica, 2009).

In plants, the data suggest that AP-3 might be involved in trafficking membrane proteins from the TGN to PSVs. For example, the δ-subunit of *Arabidopsis* AP-3 interacts with EpsinR2, a protein that binds to VTI12, clathrin, and phosphatidylinositol-3-phosphate (Lee et al., 2007). VTI12 is a vesicle-associated SNARE that localizes to the TGN in plants (Surpin et al., 2003) and has a role in protein trafficking to PSVs (Sanmartín et al., 2007). Moreover, the AP-3 δ adaptin was shown to colocalize with TERMINAL FLOWER1, which is also involved in protein trafficking to PSVs (Sohn et al., 2007). In contrast, the *ap-3* β mutant is specifically affected in the biogenesis, identity, and function of LVs, and it has been proposed that this might occur via a PVC-independent pathway (Feraru et al., 2010).

The results obtained in this article suggest an AP-3 function in plants that is similar to what has been described in yeast. In both systems, AP-3 appears to recruit cargo proteins directly from the Golgi, which is supported by the observation that GFP-SUC4 colocalizes with *cis*-Golgi markers in *ap-3* β mutants, that the labeled structures can be characterized as Golgis based on their typical shape, and that GFP-SUC4 does not enter the TGN in *ap-3* β mutants. As, finally, both the INT1 route and the SUC4 route are sensitive to BFA and therefore involve the Golgi, we propose the model shown in Figure 9. According to this model, INT1 and SUC4 enter the Golgi via the early secretory pathway from the ER. While SUC4 is then recruited as cargo by AP-3 in the *cis*-Golgi, INT1 appears to be sorted via the classical, AP-3–independent vacuolar-sorting route involving the TGN and PVCs. In addition to these two Golgi-dependent routes, a third route seems to exist for the targeting of proteins directly from the ER to the vacuolar membrane in a Golgi-independent way. This route might be similar to the sorting route that has been described for the targeting of α-TIP to PSVs (Jiang and Rogers, 1998; Park et al., 2004). Furthermore, the existence of additional, so far unidentified targeting pathways to the tonoplast cannot be excluded.

Recently, Bottanelli et al. (2011) also postulated at least three different sorting routes for membrane proteins to the tonoplast in tobacco epidermis cells. Of the three identified transport routes, one was Golgi independent, while the other two required an intact Golgi network with one of them also including the TGN. These findings are in perfect agreement with our data.

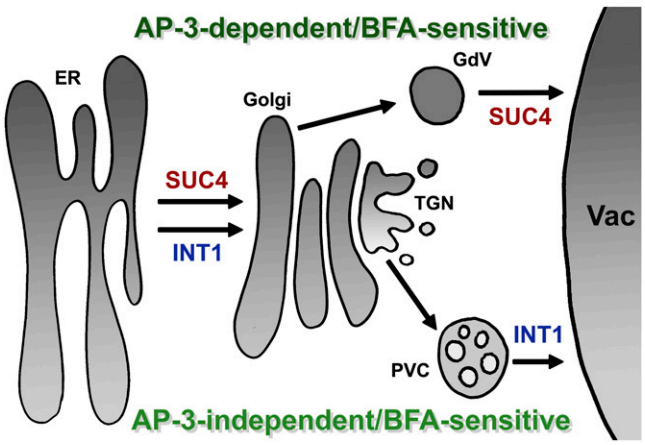

Figure 9. Model for the Alternative Sorting Routes of INT1 and SUC4.

After its synthesis in the ER, SUC4 is sorted to the Golgi, from where it reaches the tonoplast directly via an AP-3–dependent/BFA-sensitive route (GdV, Golgi-derived vesicle). By contrast, INT1 reaches the tonoplast via the classical, AP-3–independent/BFA-sensitive route that involves the TGN and the PVC. Vac, vacuole.

Outlook

The physiological reason for the existence of different sorting routes for tonoplast transporters is unclear. No sorting of SUC4 via the INT1 route is seen in the *ap-3* β mutant, indicating a strict separation of the two Golgi-dependent sorting routes and no spillover, even if one of the routes is blocked or overloaded. In analogy to the situation in yeast and animals, one could speculate that the INT1 route is responsible for the tonoplast sorting of housekeeping tonoplast proteins, while the SUC4 route might be required for tonoplast sorting in response to specific developmental or environmental conditions or of special proteins under nonstandard conditions. In fact, a specific up- or downregulation of the AP-3–dependent SUC4 route might represent a means to regulate tonoplast sorting of an entire set of membrane proteins. The identification of additional AP-3 cargo proteins will help to understand the physiological needs for this alternative sorting route in plants.

METHODS

Strains, Growth Conditions, and Plant Transformation

Arabidopsis thaliana ecotype Columbia-0 and the *ap-3* β mutant (SAIL_1258_G03 =*pat2-2*; obtained from the Nottingham Arabidopsis Stock Centre) were grown under short-day conditions (8 h light/16 h dark) at 22°C in growth chambers for preparation of mesophyll protoplasts. Stable transformants were generated with *Agrobacterium tumefaciens* strain GV3101 (Holsters et al., 1980).

Constructs for Transient and Stable Transformation

The soybean (*Glycine max*) α-1,2-mannosidase I–derived *cis*-Golgi marker CD3-967-mCherry (Saint-Jore-Dupas et al., 2006; Nelson et al., 2007) was obtained from the ABRC. Additionally, the *cis*-Golgi marker v-SNARE MEMB12 (Uemura et al., 2004) and the Golgi and TGN marker GTPase RabD1 (Pinheiro et al., 2009) were used for colocalization studies, carrying mCherry fusions in the Wave127R or Wave25R construct, respectively, published by Geldner et al. (2009).

For the domain swaps between INT1 and INT4, an internal *Nco*I site in the *Arabidopsis INT1* CDS was removed by PCR (primers INT1-pci, INT1BglN, INT1BglC, and INT1-nco; see Supplemental Table 2 online). Insertion into the vector pCS120 (Dotzauer et al., 2010) yielded the plasmid pCS143. Amplification of the *INT1* CDS from pCS143 (primers INT1-5-PciI and INT1-3-PciI) introduced *Pci*I sites at both ends and removed the stop codon. Unique *Avr*II, *Nae*I, and *Stu*I cloning sites were introduced by site-directed mutagenesis [primers INT1-AvrII-F, INT1-AvrII-R, INT1-NaeI-F, INT1-NaeI-R, INT1-StuI-F(long), and INT1-StuI-R].

The *Arabidopsis INT4* CDS was amplified with the primers INT4-pci and INT4-nco and inserted into pCS120, yielding pCS144. Amplification of the *INT4* CDS from pCS144 (primers INT4-5-NcoI and INT4-3-NcoI) introduced *Nco*I sites at both ends and removed the stop codon. Unique *Avr*II, *Nae*I, and *Stu*I cloning sites were introduced by site-directed mutagenesis [primers INT4-AvrII-F, INT4-AvrII-R, INT4-NaeI-F, INT4-NaeI-R, INT4-StuI-F(long), and INT4-StuI-R].

Domain switches with INT1 and INT4 were performed in the background of pJET1.2 (Fermentas). The N termini of INT1 and INT4 were directly exchanged via PCR using the primers INT4-N-Term-PciI or INT1-N-Term-PciI. The L1 and L4 domains and the C1 and C4 domains were exchanged using the inserted *Avr*II, *Nae*I, or *Stu*I cloning sites (see Supplemental Figure 1 online).

For the addition of the INT4 C terminus to the intact INT1 protein [INT1(C4)] or vice versa [INT4(C1)], unique *Stu*I sites were created at the 3′-end of the *INT1* CDS (primers INT1-5-PciI and INT1-3′StuI-R) or at the 3′-end of the *INT4* CDS (primers INT4-5-NcoI and INT4-3′StuI-R). The PCR fragments were cloned into pJET1.2, and the respective C termini were inserted into the *Stu*I sites.

C-terminal truncations or mutations of INT1 were created via PCR using the forward primer INT1-5-PciI and one of the following reverse primers: INT1-del9r (INT1Δ9), INT1-del30r (INT1Δ30), INT1-ER/AAr (INT1-$C_{ER\rightarrow AA}$), INT1-LLE/AAAr (INT1-$C_{LLE\rightarrow AAA}$), or INT1-LLE/SSSr ($INT1_{(LLE\rightarrow SSS)}$). C-terminal modifications of INT4 were generated with the primer INT4-5-NcoI and one of the following reverse primers: INT4-RRREKK/AAAAAAr ($INT4_{(RRREKK\rightarrow AAAAAA)}$), INT4-del23r (INT4Δ23), or INT4-FK/AAr ($INT4_{(FK\rightarrow AA)}$). For the mutation in the INT4 di-Leu motif (INT4-$C_{LLE\rightarrow AAA}$), the primers INT4-5-NcoI, INT4-LLE/AAA-R, INT4-LLE/AAA-F, and INT4-3-NcoI were used.

All chimera, truncations, and mutations of INT1 and INT4 contain flanking *Nco*I or *Pci*I cloning sites for insertion into the expression vectors. For *GFP* fusion constructs, the above-described constructs were excised from pJET1.2 with *Nco*I or *Pci*I and inserted into the unique *Nco*I cloning sites of pCS120 (Dotzauer et al., 2010) for C-terminal GFP fusions or pSS87 (Schneider et al., 2011) for N-terminal GFP fusions.

To create chimeric fusions of SUC2 and SWEET1 to the INT1 C terminus, derivatives of pCS120 and pSS87 with the CDS of the INT1 C terminus and a unique *Nco*I cloning site at the 5′-end were established. To this end, the *INT1* C-terminal sequence was amplified with a 5′ *Nco*I site and a 3′ *Pci*I site (primers C-INT1-NcoI-5 and INT1-3-PciI). The fragment was inserted into pCS120, yielding an NcoI/INT1-C terminus/GFP cassette in plasmid pSW110, or into pSS87, yielding a GFP/NcoI/INT1 C terminus cassette in plasmid pSW111.

For chimeric SUC2 proteins, the *SUC2* CDS was amplified (primers SUC2-5-PciI and SUC2-3-PciI), the stop codon was removed, and flanking *Pci*I sites were introduced. The sequence was inserted into pSS87, yielding GFP-SUC2; into pCS120, yielding SUC2-GFP; into pSW111, yielding GFP-SUC2(C1); and into pSW110, yielding SUC2(C1)-GFP. The shorter *SUC2Δ14* sequence with flanking *Pci*I sites (primers SUC2-5-PciI and SUC2-3-PciI wo C-Term) was inserted into the *Nco*I site of pSW110, yielding SUC2Δ14(C1)-GFP; into pSW111, yielding GFP-SUC2Δ14(C1); into pCS120, yielding SUC2Δ14-GFP; or into pSS87, yielding GFP-SUC2Δ14. To obtain $SUC2\Delta14(C1)_{(LLE\rightarrow AAA)}$, PCR was performed with the primers SUC2-5-PciI and INT1-LLE/AAAr, using GFP-SUC2Δ14(C1) as template. The resulting sequence was inserted into pSS87, yielding GFP-$SUC2\Delta14(C1)_{(LLE\rightarrow AAA)}$.

For chimeric SWEET1 proteins, the *SWEET1* CDS was amplified (primers SWEET1-5-NcoI and SWEET1-3-NcoI), the stop codon was removed, and flanking *Nco*I sites were introduced. The sequence was inserted into pSS87, yielding GFP-SWEET1; into pCS120, yielding SWEET1-GFP; and into pSW111, yielding GFP-SWEET(C1). The shorter *SWEET1Δ33* sequence with flanking *Nco*I sites (primers SWEET1-5-NcoI and SWEET1 wo C-Term-3-NcoI) was inserted into the *Nco*I site of pSS87, yielding GFP-SWEET1Δ33; or pSW111, yielding GFP-SWEET1Δ33(C1).

To generate GFP-SUC4, the *Arabidopsis SUC4* CDS was amplified (primers SUC4-PciI-F and SUC4-StuI-PciI-R). Flanking *Pci*I cloning sites were introduced for insertion into pSS87 and a 3′ *Stu*I site for the insertion of the INT1 C terminus to generate GFP-SUC4(C1).

To generate ESL1-GFP, the *ESL1* CDS was amplified (primers ERD6B5 and ERD6B3), and the PCR product was cloned into pENTR/D-TOPO (Invitrogen) and then introduced into the destination vector pK7FWG2,0 (Karimi et al., 2002) by Gateway cloning.

For all fusions, the modified *Aequorea victoria* sGFP(S65T) was used (Heim et al., 1995).

Treatment with BFA

Treatment with BFA was performed as described by Isayenkov et al. (2011) with minor modifications: a 10 mg mL^{-1} stock solution of BFA (Sigma-Aldrich) in DMSO was added to protoplasts to a final concentration of 25 μg

mL^{-1} 1 h after transformation. In all analyses, the same amount of DMSO without BFA was used as control. For recovery experiments, the protoplasts were washed and transferred to buffer without BFA.

Complementation of an *int1* Mutant

As used for previous experiments (Schneider et al., 2008), a 1210-bp *INT1* promoter fragment with a *Hin*dIII site at the 5′-end and an *Sbf*I site at the 3′-end was amplified (primers INT1-p5 and pINT1-3′-SbfI) and inserted into the respective sites of the plant transformation vector pAF16 (Stadler et al., 2005), yielding pINT1-pAF16. The *INT4ΔC(C1)* cDNA was amplified (primers INT4-5′-SbfI and INT1-3′-stop-XbaI) from the plasmid containing this sequence for sorting analyses, introducing an *Sbf*I site at the 5′-end and a *Xba*I site at the 3′-end, allowing the insertion into pINT1-pAF16 and yielding plasmid pSS100 [p*INT1/INT4ΔC(C1)*]. After transformation, growth of wild-type, *int1*, and *int1/INT4ΔC(C1)* plants was compared under long-day growth conditions on plates in upright position.

Protoplast Isolation, Polyethylene Glycol–Mediated Transformation of Protoplasts, and Osmotic Lysis of Plasma Membranes

Arabidopsis mesophyll protoplasts were generated (Drechsel et al., 2011) and transformed (Abel and Theologis, 1994) as described. Transformed *Arabidopsis* protoplasts were incubated for 24 to 72 h in the dark at 22°C prior to confocal analysis. Osmotic lysis of protoplasts was performed as described by Schneider et al. (2011).

Confocal Microscopy

Images of protoplasts were taken on a confocal laser scanning microscope (Leica TCS SPII; Leica Microsystems) using 488-nm (GFP) and 543-nm (RFP and mCherry) laser light for excitation and processed with Leica Confocal Software 2.5. Detection windows ranged from 495 to 556 nm for GFP and from 565 to 632 nm for RFP and mCherry.

Protein Extraction and Immunoblot Analysis

Membrane and soluble proteins were isolated from transiently transformed *Arabidopsis* protoplasts (He et al., 1996), with some modifications. Separation of membrane and soluble proteins was performed by ultracentrifugation at 100,000*g* for 1 h at 4°C. The supernatant was used as source for soluble proteins, and the pellet containing total membrane proteins was dissolved in membrane protein buffer consisting of 50 mM K_3PO_4, pH 6.3, 20% glycerol, and 1 mM EDTA. Extracts of soluble and membrane proteins were mixed with SDS sample buffer (250 mM Tris-HCl, pH 6.8, 20% β-mercaptoethanol, 8% SDS, 0.04% bromophenol blue, and 20% glycerol), and samples with soluble proteins were boiled for 5 min. Proteins were separated by SDS-PAGE and transferred to nitrocellulose membranes using protein electrophoresis and blotting apparatuses (Bio-Rad). Blots were developed using a Lumi-LightPLUS Western Blotting Kit (Roche) and visualized by Kodak BioMax XAR film. Anti-GFP antibodies conjugated with horseradish peroxidase were used as described by the manufacturer (Invitrogen).

Accession Numbers

Sequence data from this article can be found in the Arabidopsis Genome Initiative or GenBank/EMBL databases under the following accession numbers: INT1 (At2g43330), INT4 (At4g16480), SUC2 (At1g22710), SUC4 (At1g09960), SWEET1 (At1g21460), ESL1 (At1g08920), AP-3 (At3g55480), Man1 (AF126550), MEMB12 (At5g50440), and RabD1 (At3g11730).

Supplemental Data

The following materials are available in the online version of this article.

Supplemental Figure 1. *Arabidopsis INT1* and *INT4* Coding Sequences and Modifications Introduced to Allow Domain Swapping.

Supplemental Figure 2. Immunoblot Analyses to Reveal Intactness of GFP Fusion Proteins in Transformed *Arabidopsis* Protoplasts.

Supplemental Figure 3. Subcellular Localization of INT1ΔC(C4)-GFP and INT4ΔC(C1)-GFP.

Supplemental Figure 4. Subcellular Localization of GFP-INT4(C1) and GFP-INT1(C4).

Supplemental Figure 5. Subcellular Localization of GFP-INT1$_{(LLE \rightarrow SSS)}$.

Supplemental Figure 6. Subcellular Localization of SWEET1-GFP and GFP-SWEET1 Analyzed 72 h after Transformation.

Supplemental Figure 7. Unrooted Phylogenetic Tree of AP Complex β-Subunits and Related Proteins from Human, Yeast, and *Arabidopsis*.

Supplemental Figure 8. Colocalization of GFP-SUC4 and the *cis*-Golgi Marker Wave127R in *ap-3* β Protoplasts.

Supplemental Figure 9. Colocalization of GFP-SUC4 and the Golgi/TGN Marker Wave25R in *ap-3* β Protoplasts.

Supplemental Figure 10. Colocalization of GFP-SUC4 and the *cis*-Golgi Marker CD3-967-mCherry in a Wild-Type Protoplast and Effect of BFA on a *GFP-SUC4*–Expressing Protoplast.

Supplemental Figure 11. Reestablishment of the Original Subcellular Localization for INT4, INT1, and SUC4 in BFA-Treated Protoplasts after Removal of BFA.

Supplemental Table 1. Quantification of the Subcellular Localizations Seen with the Different Constructs Analyzed.

Supplemental Table 2. List of Primers Used in This Work.

Supplemental Data Set 1. Sequence Alignment Used for the Calculation of the Tree Shown in Figure 7.

ACKNOWLEDGMENTS

This work was supported by a grant of the German Research Foundation to N.S. (Deutsche Forschungsgemeinshaft Research Unit 1061, SA 382/20). We thank Karin Schumacher (University of Heidelberg, Germany) for the Wave 25R and Wave127R constructs and for helpful discussions, as well as Magdalena Weingartner (University of Erlangen-Nürnberg, Germany) for critical comments on the manuscript.

AUTHOR CONTRIBUTIONS

N.S. designed the work. S.W., P.W., D.D., and S.S. performed research. S.W., S.S., and N.S. analyzed the data. S.W. and N.S. wrote the article.

Received August 12, 2011; revised December 22, 2011; accepted December 28, 2011; published January 17, 2012.

REFERENCES

Abel, S., and Theologis, A. (1994). Transient transformation of *Arabidopsis* leaf protoplasts: A versatile experimental system to study gene expression. Plant J. **5:** 421–427.

Bassham, D.C., Brandizzi, F., Otegui, M., and Sanderfoot, A.A. (2008). The secretory system of *Arabidopsis*. The *Arabidopsis* Book, American Society of Plant Biologists **6:** e0116, doi/10.1199/tab.0116.

Bednarek, S.Y., and Raikhel, N.V. (1992). Intracellular trafficking of secretory proteins. Plant Mol. Biol. **20:** 133–150.

Bonifacino, J.S., and Traub, L.M. (2003). Signals for sorting of transmembrane proteins to endosomes and lysosomes. Annu. Rev. Biochem. **72:** 395–447.

Bork, P., Doerks, T., Springer, T.A., and Snel, B. (1999). Domains in plexins: Links to integrins and transcription factors. Trends Biochem. Sci. **24:** 261–263.

Bottanelli, F., Foresti, O., Hanton, S., and Denecke, J. (2011). Vacuolar transport in tobacco leaf epidermis cells involves a single route for soluble cargo and multiple routes for membrane cargo. Plant Cell **23:** 3007–3025.

Brandizzi, F., Frangne, N., Marc-Martin, S., Hawes, C., Neuhaus, J.-M., and Paris, N. (2002). The destination for single-pass membrane proteins is influenced markedly by the length of the hydrophobic domain. Plant Cell **14:** 1077–1092.

Cai, Y., Jia, T., Lam, S.K., Ding, Y., Gao, C., San, M.W., Pimpl, P., and Jiang, L. (2011). Multiple cytosolic and transmembrane determinants are required for the trafficking of SCAMP1 via an ER-Golgi-TGN-PM pathway. Plant J. **65:** 882–896.

Chen, L.Q., et al. (2010). Sugar transporters for intercellular exchange and nutrition of pathogens. Nature **468:** 527–532.

Chrispeels, M.J. (1991). Sorting of proteins in the secretory system. Annu. Rev. Plant Physiol. Plant Mol. Biol. **42:** 1–24.

Cowles, C.R., Odorizzi, G., Payne, G.S., and Emr, S.D. (1997a). The AP-3 adaptor complex is essential for cargo-selective transport to the yeast vacuole. Cell **91:** 109–118.

Cowles, C.R., Snyder, W.B., Burd, C.G., and Emr, S.D. (1997b). Novel Golgi to vacuole delivery pathway in yeast: Identification of a sorting determinant and required transport component. EMBO J. **16:** 2769–2782.

daSilva, L.L., Foresti, O., and Denecke, J. (2006). Targeting of the plant vacuolar sorting receptor BP80 is dependent on multiple sorting signals in the cytosolic tail. Plant Cell **18:** 1477–1497.

Dell'Angelica, E.C. (2009). AP-3-dependent trafficking and disease: The first decade. Curr. Opin. Cell Biol. **21:** 552–559.

Dell'Angelica, E.C., Shotelersuk, V., Aguilar, R.C., Gahl, W.A., and Bonifacino, J.S. (1999). Altered trafficking of lysosomal proteins in Hermansky-Pudlak syndrome due to mutations in the β 3A subunit of the AP-3 adaptor. Mol. Cell **3:** 11–21.

Dhonukshe, P., Aniento, F., Hwang, I., Robinson, D.G., Mravec, J., Stierhof, Y.-D., and Friml, J. (2007). Clathrin-mediated constitutive endocytosis of PIN auxin efflux carriers in *Arabidopsis*. Curr. Biol. **17:** 520–527.

Dotzauer, D., Wolfenstetter, S., Eibert, D., Schneider, S., Dietrich, P., and Sauer, N. (2010). Novel PSI domains in plant and animal H^+-inositol symporters. Traffic **11:** 767–781.

Drechsel, G., Bergler, J., Wippel, K., Sauer, N., Vogelmann, K., and Hoth, S. (2011). C-terminal armadillo repeats are essential and sufficient for association of the plant U-box armadillo E3 ubiquitin ligase SAUL1 with the plasma membrane. J. Exp. Bot. **62:** 775–785.

Dunkel, M., Latz, A., Schumacher, K., Müller, T., Becker, D., and Hedrich, R. (2008). Targeting of vacuolar membrane localized members of the TPK channel family. Mol. Plant **1:** 938–949.

Endler, A., Meyer, S., Schelbert, S., Schneider, T., Weschke, W., Peters, S.W., Keller, F., Baginsky, S., Martinoia, E., and Schmidt, U.G. (2006). Identification of a vacuolar sucrose transporter in barley and Arabidopsis mesophyll cells by a tonoplast proteomic approach. Plant Physiol. **141:** 196–207.

Feraru, E., Paciorek, T., Feraru, M.I., Zwiewka, M., De Groodt, R., De Rycke, R., Kleine-Vehn, J., and Friml, J. (2010). The AP-3 β adaptin mediates the biogenesis and function of lytic vacuoles in *Arabidopsis*. Plant Cell **22:** 2812–2824.

Foresti, O., Gershlick, D.C., Bottanelli, F., Hummel, E., Hawes, C., and Denecke, J. (2010). A recycling-defective vacuolar sorting receptor reveals an intermediate compartment situated between prevacuoles and vacuoles in tobacco. Plant Cell **22:** 3992–4008.

Frigerio, L., Hinz, G., and Robinson, D.G. (2008). Multiple vacuoles in plant cells: Rule or exception? Traffic **9:** 1564–1570.

Gasber, A., Klaumann, S., Trentmann, O., Trampczynska, A., Clemens, S., Schneider, S., Sauer, N., Feifer, I., Bittner, F., Mendel, R.R., and Neuhaus, H.E. (2011). Identification of an *Arabidopsis* solute carrier critical for intracellular transport and inter-organ allocation of molybdate. Plant Biol. (Stuttg.) **13:** 710–718.

Geisler, C., Dietrich, J., Nielsen, B.L., Kastrup, J., Lauritsen, J.P.H., Ødum, N., and Christensen, M.D. (1998). Leucine-based receptor sorting motifs are dependent on the spacing relative to the plasma membrane. J. Biol. Chem. **273:** 21316–21323.

Geldner, N., Dénervaud-Tendon, V., Hyman, D.L., Mayer, U., Stierhof, Y.-D., and Chory, J. (2009). Rapid, combinatorial analysis of membrane compartments in intact plants with a multicolor marker set. Plant J. **59:** 169–178.

Gomez, L., and Chrispeels, M.J. (1993). Tonoplast and soluble vacuolar proteins are targeted by different mechanisms. Plant Cell **5:** 1113–1124.

Gu, F., Crump, C.M., and Thomas, G. (2001). Trans-Golgi network sorting. Cell. Mol. Life Sci. **58:** 1067–1084.

Hanton, S.L., Bortolotti, L.E., Renna, L., Stefano, G., and Brandizzi, F. (2005a). Crossing the divide—Transport between the endoplasmic reticulum and Golgi apparatus in plants. Traffic **6:** 267–277.

Hanton, S.L., Renna, L., Bortolotti, L.E., Chatre, L., Stefano, G., and Brandizzi, F. (2005b). Diacidic motifs influence the export of transmembrane proteins from the endoplasmic reticulum in plant cells. Plant Cell **17:** 3081–3093.

He, Z.H., Fujiki, M., and Kohorn, B.D. (1996). A cell wall-associated, receptor-like protein kinase. J. Biol. Chem. **271:** 19789–19793.

Heim, R., Cubitt, A.B., and Tsien, R.Y. (1995). Improved green fluorescence. Nature **373:** 663–664.

Höfte, H., and Chrispeels, M.J. (1992). Protein sorting to the vacuolar membrane. Plant Cell **4:** 995–1004.

Holsters, M., Silva, B., Van Vliet, F., Genetello, C., De Block, M., Dhaese, P., Depicker, A., Inzé, D., Engler, G., Villarroel, R., Van Montagu, M., and Schell, J. (1980). The functional organization of the nopaline *A. tumefaciens* plasmid pTiC58. Plasmid **3:** 212–230.

Hwang, I., and Robinson, D.G. (2009). Transport vesicle formation in plant cells. Curr. Opin. Plant Biol. **12:** 660–669.

Isayenkov, S., Isner, J.C., and Maathuis, F.J.M. (2010). Vacuolar ion channels: Roles in plant nutrition and signalling. FEBS Lett. **584:** 1982–1988.

Isayenkov, S., Isner, J.C., and Maathuis, F.J.M. (2011). Rice two-pore K^+ channels are expressed in different types of vacuoles. Plant Cell **23:** 756–768.

Jiang, L., and Rogers, J.C. (1998). Integral membrane protein sorting to vacuoles in plant cells: Evidence for two pathways. J. Cell Biol. **143:** 1183–1199.

Karimi, M., Inzé, D., and Depicker, A. (2002). GATEWAY vectors for Agrobacterium-mediated plant transformation. Trends Plant Sci. **7:** 193–195.

Kirchhausen, T. (1999). Adaptors for clathrin-mediated traffic. Annu. Rev. Cell Dev. Biol. **15:** 705–732.

Langhans, M., Hawes, C., Hillmer, S., Hummel, E., and Robinson, D.G. (2007). Golgi regeneration after brefeldin A treatment in BY-2 cells entails stack enlargement and cisternal growth followed by division. Plant Physiol. **145:** 527–538.

Lee, G.-J., Kim, H., Kang, H., Jang, M., Lee, D.W., Lee, S., and Hwang, I. (2007). EpsinR2 interacts with clathrin, adaptor protein-3, AtVTI12, and phosphatidylinositol-3-phosphate. Implications for EpsinR2 function in protein trafficking in plant cells. Plant Physiol. **143:** 1561–1575.

Letourneur, F., and Klausner, R.D. (1992). A novel di-leucine motif and a tyrosine-based motif independently mediate lysosomal targeting and endocytosis of CD3 chains. Cell **69:** 1143–1157.

Lloyd, V., Ramaswami, M., and Krämer, H. (1998). Not just pretty eyes: Drosophila eye-colour mutations and lysosomal delivery. Trends Cell Biol. **8:** 257–259.

Maîtrejean, M., Wudick, M.M., Voelker, C., Prinsi, B., Mueller-Roeber, B., Czempinski, K., Pedrazzini, E., and Vitale, A. (2011). Assembly and sorting of the tonoplast potassium channel AtTPK1 and its turnover by internalization into the vacuole. Plant Physiol. **156:** 1783–1796.

Marger, M.D., and Saier, M.H., Jr. (1993). A major superfamily of transmembrane facilitators that catalyse uniport, symport and antiport. Trends Biochem. Sci. **18:** 13–20.

Martinoia, E., Maeshima, M., and Neuhaus, H.E. (2007). Vacuolar transporters and their essential role in plant metabolism. J. Exp. Bot. **58:** 83–102.

Marty, F. (1999). Plant vacuoles. Plant Cell **11:** 587–600.

Nebenführ, A., Ritzenthaler, C., and Robinson, D.G. (2002). Brefeldin A: Deciphering an enigmatic inhibitor of secretion. Plant Physiol. **130:** 1102–1108.

Nelson, B.K., Cai, X., and Nebenführ, A. (2007). A multicolored set of in vivo organelle markers for co-localization studies in *Arabidopsis* and other plants. Plant J. **51:** 1126–1136.

Neuhaus, H.E. (2007). Transport of primary metabolites across the plant vacuolar membrane. FEBS Lett. **581:** 2223–2226.

Odorizzi, G., Cowles, C.R., and Emr, S.D. (1998). The AP-3 complex: A coat of many colours. Trends Cell Biol. **8:** 282–288.

Ortiz-Zapater, E., Soriano-Ortega, E., Marcote, M.J., Ortiz-Masiá, D., and Aniento, F. (2006). Trafficking of the human transferrin receptor in plant cells: Effects of tyrphostin A23 and brefeldin A. Plant J. **48:** 757–770.

Pandey, K.N. (2010). Small peptide recognition sequence for intracellular sorting. Curr. Opin. Biotechnol. **21:** 611–620.

Paris, N., Stanley, C.M., Jones, R.L., and Rogers, J.C. (1996). Plant cells contain two functionally distinct vacuolar compartments. Cell **85:** 563–572.

Park, M., Kim, S.J., Vitale, A., and Hwang, I. (2004). Identification of the protein storage vacuole and protein targeting to the vacuole in leaf cells of three plant species. Plant Physiol. **134:** 625–639.

Pinheiro, H., Samalova, M., Geldner, N., Chory, J., Martinez, A., and Moore, I. (2009). Genetic evidence that the higher plant Rab-D1 and Rab-D2 GTPases exhibit distinct but overlapping interactions in the early secretory pathway. J. Cell Sci. **122:** 3749–3758.

Robinson, M.S. (2004). Adaptable adaptors for coated vesicles. Trends Cell Biol. **14:** 167–174.

Saint-Jean, B., Seveno-Carpentier, E., Alcon, C., Neuhaus, J.M., and Paris, N. (2010). The cytosolic tail dipeptide Ile-Met of the pea receptor BP80 is required for recycling from the prevacuole and for endocytosis. Plant Cell **22:** 2825–2837.

Saint-Jore-Dupas, C., Nebenführ, A., Boulaflous, A., Follet-Gueye, M.-L., Plasson, C., Hawes, C., Driouich, A., Faye, L., and Gomord, V. (2006). Plant N-glycan processing enzymes employ different targeting mechanisms for their spatial arrangement along the secretory pathway. Plant Cell **18:** 3182–3200.

Sandoval, I.V., Martínez-Arca, S., Valdueza, J., Palacios, S., and Holman, G.D. (2000). Distinct reading of different structural determinants modulates the dileucine-mediated transport steps of the lysosomal membrane protein LIMPII and the insulin-sensitive glucose transporter GLUT4. J. Biol. Chem. **275:** 39874–39885.

Sanmartín, M., Ordóñez, A., Sohn, E.J., Robert, S., Sánchez-Serrano, J.J., Surpin, M.A., Raikhel, N.V., and Rojo, E. (2007). Divergent functions of VTI12 and VTI11 in trafficking to storage and lytic vacuoles in *Arabidopsis*. Proc. Natl. Acad. Sci. USA **104:** 3645–3650.

Sauer, N., and Stolz, J. (1994). SUC1 and SUC2: Two sucrose transporters from *Arabidopsis thaliana*; expression and characterization in baker's yeast and identification of the histidine-tagged protein. Plant J. **6:** 67–77.

Schneider, S., Beyhl, D., Hedrich, R., and Sauer, N. (2008). Functional and physiological characterization of *Arabidopsis* INOSITOL TRANSPORTER1, a novel tonoplast-localized transporter for *myo*-inositol. Plant Cell **20:** 1073–1087.

Schneider, S., Hulpke, S., Schulz, A., Yaron, I., Höll, J., Imlau, A., Schmitt, B., Batz, S., Wolf, S., Hedrich, R., and Sauer, N. (2011). Vacuoles release sucrose via tonoplast-localized SUC4-type transporters. Plant Biol. (Stuttg.) http://dx.doi.org/10.1111/j.1438-8677.2011.00506.x.

Schneider, S., Schneidereit, A., Konrad, K.R., Hajirezaei, M.-R., Gramann, M., Hedrich, R., and Sauer, N. (2006). Arabidopsis INOSITOL TRANSPORTER4 mediates high-affinity H+ symport of myo-inositol across the plasma membrane. Plant Physiol. **141:** 565–577.

Schulz, A., Beyhl, D., Marten, I., Wormit, A., Neuhaus, E., Poschet, G., Büttner, M., Schneider, S., Sauer, N., and Hedrich, R. (2011). Proton-driven sucrose symport and antiport are provided by the vacuolar transporters SUC4 and TMT1/2. Plant J. **68:** 129–136.

Scott, G.K., Gu, F., Crump, C.M., Thomas, L., Wan, L., Xiang, Y., and Thomas, G. (2003). The phosphorylation state of an autoregulatory domain controls PACS-1-directed protein traffic. EMBO J. **22:** 6234–6244.

Sohn, E.J., Rojas-Pierce, M., Pan, S., Carter, C., Serrano-Mislata, A., Madueño, F., Rojo, E., Surpin, M., and Raikhel, N.V. (2007). The shoot meristem identity gene TFL1 is involved in flower development and trafficking to the protein storage vacuole. Proc. Natl. Acad. Sci. USA **104:** 18801–18806.

Sorieul, M., Santoni, V., Maurel, C., and Luu, D.T. (2011). Mechanisms and effects of retention of over-expressed aquaporin AtPIP2;1 in the endoplasmic reticulum. Traffic **12:** 473–482.

Stadler, R., and Sauer, N. (1996). The *Arabidopsis thaliana AtSUC2* gene is specifically expressed in companion cells. Bot. Acta **109:** 299–306.

Stadler, R., Wright, K.M., Lauterbach, C., Amon, G., Gahrtz, M., Feuerstein, A., Oparka, K.J., and Sauer, N. (2005). Expression of GFP-fusions in *Arabidopsis* companion cells reveals non-specific protein trafficking into sieve elements and identifies a novel post-phloem domain in roots. Plant J. **41:** 319–331.

Surpin, M., Zheng, H., Morita, M.T., Saito, C., Avila, E., Blakeslee, J.J., Bandyopadhyay, A., Kovaleva, V., Carter, D., Murphy, A., Tasaka, M., and Raikhel, N. (2003). The VTI family of SNARE proteins is necessary for plant viability and mediates different protein transport pathways. Plant Cell **15:** 2885–2899.

Takano, J., Tanaka, M., Toyoda, A., Miwa, K., Kasai, K., Fuji, K., Onouchi, H., Naito, S., and Fujiwara, T. (2010). Polar localization and degradation of *Arabidopsis* boron transporters through distinct trafficking pathways. Proc. Natl. Acad. Sci. USA **107:** 5220–5225.

Truernit, E., and Sauer, N. (1995). The promoter of the *Arabidopsis thaliana* SUC2 sucrose-H^+ symporter gene directs expression of beta-glucuronidase to the phloem: Evidence for phloem loading and unloading by SUC2. Planta **196:** 564–570.

Uemura, T., Sato, M.H., and Takeyasu, K. (2005). The longin domain regulates subcellular targeting of VAMP7 in *Arabidopsis thaliana*. FEBS Lett. **579:** 2842–2846.

Uemura, T., Ueda, T., Ohniwa, R.L., Nakano, A., Takeyasu, K., and Sato, M.H. (2004). Systematic analysis of SNARE molecules in *Arabidopsis*: Dissection of the post-Golgi network in plant cells. Cell Struct. Funct. **29:** 49–65.

Waites, C.L., Mehta, A., Tan, P.K., Thomas, G., Edwards, R.H., and Krantz, D.E. (2001). An acidic motif retains vesicular monoamine

transporter 2 on large dense core vesicles. J. Cell Biol. **152:** 1159–1168.

Wormit, A., Trentmann, O., Feifer, I., Lohr, C., Tjaden, J., Meyer, S., Schmidt, U., Martinoia, E., and Neuhaus, H.E. (2006). Molecular identification and physiological characterization of a novel monosaccharide transporter from *Arabidopsis* involved in vacuolar sugar transport. Plant Cell **18:** 3476–3490.

Yamada, K., Osakabe, Y., Mizoi, J., Nakashima, K., Fujita, Y., Shinozaki, K., and Yamaguchi-Shinozaki, K. (2010). Functional analysis of an *Arabidopsis thaliana* abiotic stress-inducible facilitated diffusion transporter for monosaccharides. J. Biol. Chem. **285:** 1138–1146.

Zelazny, E., Miecielica, U., Borst, J.W., Hemminga, M.A., and Chaumont, F. (2009). An N-terminal diacidic motif is required for the trafficking of maize aquaporins ZmPIP2;4 and ZmPIP2;5 to the plasma membrane. Plant J. **57:** 346–355.

Zwiewka, M., Feraru, E., Möller, B., Hwang, I., Feraru, M.I., Kleine-Vehn, J., Weijers, D., and Friml J. (2011). The AP-3 adaptor complex is required for vacuolar function in *Arabidopsis*. Cell Res. **21:** 1711–1722.